column (5 × 30 cm, benzene) and eluted with benzene. After unreacted benzoate **2** passed through the column, elution with benzene/ether (50/1) eluted the desired dibenzoate. Removal of the solvent gave white crystals, yield 1.8 g (19%): mp 128-129 °C; ^{1}H NMR ($CDCl_3$) δ 1.37 (t, 6 H), 1.6-2.0 (br m, 12 H), 4.06 (t, 8 H), 4.34 (q, 4 H), 6.58 (t, 2 H), 7.14 (d, 4 H).

3,3',5,5'-Bis(1,5-pentanediyldioxy)dibenzoic Acid (3b). To a solution of 1.65 g (3.65 mmol) of the precursor diester **3a** in 50 mL of acetone was added a solution of 4.0 g of NaOH in 40 mL of H_2O. The mixture was then stirred for 30 min at 40 °C. To the solution was added 2 N HCl until the pH of the mixture was lowered to about 2; then a white precipitate was obtained. The solid was filtered off, washed well with H_2O, and dried at 80 °C under vacuum; yield 1.40 g (97%): mp 280-283 °C dec; ^{1}H NMR (D_2O/K_2CO_3) δ 1.4-1.8 (br m, 12 H), 4.81 (br s, 8 H), 6.45 (s, 2 H), 7.05 (d, 4 H).

3,3',5,5'-Bis(1,5-pentanediyldioxy)dibenzoyl Chloride (3c). The precursor diacid **3b** (1.40 g, 3.53 mmol) was heated at reflux for 3 h in 20 mL of $SOCl_2$ containing a drop of DMF. Removal of excess $SOCl_2$ from the mixture under vacuum gave a pale yellow solid, yield 1.45 g (95%): mp 144-147 °C; ^{1}H NMR ($CHCl_3$) δ 1.38 (m, 4 H), 1.78 (m, 8 H), 4.07 (t, 8 H), 6.67 (t, 2 H), 7.19 (d, 4 H).

Bis-Roof Porphyrin, H_2(BRP). To a solution of 0.36 g (0.53 mmol) of α,β,α,β-*meso*-tetrakis(*o*-aminophenyl)porphyrin in 500 mL of dry CH_2Cl_2 containing 0.5 mL of *N*-methylmorpholine in an ice bath was added a solution of 0.50 g (1.2 mmol) of the diacid chloride, **3c**, in 100 mL of dry CH_2Cl_2. The solution was then stirred for 20 h at that temperature. After the volume of the reactant was reduced to 200 mL, the organic solution was washed twice with H_2O and then dried over anhydrous Na_2SO_4. After filtration, the solution was evaporated to dryness. The residue was purified by silica-gel column chromatography (benzene, 3 × 35 cm) and elution with benzene/acetone (30/1), yielding the desired porphyrin, 0.27 g (32%): ^{1}H NMR ($CDCl_3$) δ -3.17 (s, 2 H), 1.02 (m, 8 H), 1.29 (m, 16 H), 3.44 (s, 16 H), 5.84 (t, 4 H), 5.94 (d, 8 H), 6.86 (s, 4 H), 7.60 (t, 4 H), 7.91 (t, 4 H), 8.05 (d, 4 H), 8.43 (d, 4 H), 8.89 (s, 8 H); vis ($CHCl_3$) λ 402 (sh), 421.8 (Soret), 482 (sh), 515.0, 548.8, 587.4, 642.5 nm. Anal. Calcd for $C_{92}H_{82}N_8O_{12}\cdot CHCl_3$: C, 69.33; H, 5.19; N, 6.96. Found: C, 69.98; H, 5.49; N, 7.24.

Zinc Bis-Roof Porphyrin, Zn(BRP). To a solution of 0.11 g (0.068 mmol) of H_2(BRP) in 20 mL of THF was added 0.20 g of $ZnCl_2$ and 0.1 mL of 2,6-lutidine. After being refluxed for 6 h, the reaction mixture was evaporated; then the residue was dissolved in 100 mL of chloroform. The organic layer was washed twice with 200 mL of H_2O and dried over anhydrous Na_2SO_4. After removal of the solvent, the solid was purified on a silica-gel column ($CHCl_3$, 3 × 25 cm), eluting with chloroform/ether (10/1); yield 0.11 g (95%): ^{1}H NMR ($CDCl_3$) δ 1.03 (m, 8 H), 1.30 (m, 16 H), 3.38 (s, 16 H), 5.81 (t, 4 H), 5.87 (s, 8 H), 6.98 (s, 4 H), 7.59 (t, 4 H), 7.88 (t, 4 H), 8.13 (d, 4 H), 8.39 (d, 4 H), 8.91 (s, 8 H); vis (toluene) λ 430.0 (Soret), 553.6, 590.4 nm; vis ($CHCl_3$) λ 422.5 (Soret), 548.5, 585 (sh) nm. Anal. Calcd for $C_{92}H_{80}N_8O_{12}\cdot CHCl_3\cdot 2H_2O$: C, 65.30; H, 5.01; N, 6.55. Found: C, 65.73; H, 5.03; N, 6.18.

Acknowledgment. This work was supported by a Grant-in-Aid for Scientific Research from the Ministry of Education (No. 03640530). We also thank Dr. H. Kizu for recording the 400-MHz ^{1}H NMR spectra.

Supplementary Material Available: Table SI, giving equilibrium data for the binding of azetidine and butylamine, and Figure S1, showing the 400-MHz ^{1}H NMR spectrum for H_2(BRP) in $CDCl_3$ (2 pages). Ordering information is given on any current masthead page.

The Question of Metal-Metal Bonding in Edge-Sharing Bioctahedral Mo(III) Complexes. Variable Temperature ^{1}H NMR Study of $Mo_2Cl_6(PMe_xEt_{3-x})_4$ (x = 0-3) and the Mechanism of the Face-Sharing to Edge-Sharing Transformation

Rinaldo Poli* and John C. Gordon

Contribution from the Department of Chemistry and Biochemistry, University of Maryland, College Park, Maryland 20742. *Received February 3, 1992*

Abstract: Homoleptic (L = L') and heteroleptic (L ≠ L') edge-sharing bioctahedral Mo(III) complexes of formula $Mo_2Cl_6L_{4-n}L'_n$ (n = 0-2; L, L' = PMe_xEt_{3-x}; x = 0-3) have been generated in solution and investigated by paramagnetic ^{1}H NMR spectroscopy. The derivatives have been obtained by interaction of a face-sharing bioctahedral $Mo_2Cl_6L_3$ precursor with L' or, for the case of n = 0, L = L' = $PMeEt_2$, by brief reflux of $MoCl_3(THF)_3$ and 2 equiv of the phosphine in toluene. The $Mo_2Cl_6L_3/L'$ interaction occurs regioselectively to afford a single product, and this is followed by other processes, one of them being ligand exchange to generate a single stereoisomer of formula $Mo_2Cl_6L_2L'_2$. A relatively simple mechanistic scheme which is based on the previously proven higher trans effect of phosphine ligands with respect to chlorides for pseudooctahedral Mo(III) coordination compounds allows a rationalization of all stereochemical results. The paramagnetic shift of the phosphine proton resonances for the edge-sharing bioctahedral $Mo_2Cl_6L_{4-n}L'_n$ compounds increases as the Me/Et ratio for the phosphine substituents decreases, and it is found in general that, for a given Me/Et ratio, the system is more paramagnetic when more ethyl groups are located on equatorial phosphines. For instance, $Mo_2Cl_6(PEt_3)_2(ax\text{-}PMe_3)_2$ is more paramagnetic than the isomeric $Mo_2Cl_6(PMe_3)_2(ax\text{-}PEt_3)_2$. Variable temperature ^{1}H NMR measurements have been carried out for $Mo_2Cl_6(PMe_xEt_{3-x})_4$ (x = 0-3) and for $Mo_2Cl_6(PEt_3)_{4-n}(ax\text{-}PMe_3)_n$ (n = 1, 2). These investigations allow considerations on the ground electronic structure of these materials to be made.

Introduction

We have recently discovered a tremendous effect of minor changes in the nature of phosphine substituents on the ability of the Mo atoms in edge-sharing bioctahedral (ESBO) $Mo_2Cl_6(PR_3)_4$ to bind to each other.[1] When PR_3 = PEt_3, the two metals are separated by 3.730 (1) Å,[2] indicating no direct bonding interaction and the metals are communicating only through a weak antiferromagnetic coupling, whereas when PR_3 = PMe_2Ph, the two metals are separated by 2.8036 (8) Å, and the compound is almost completely diamagnetic, consistent with the pairing of the six metal

(1) Poli, R.; Mui, H. D. *Inorg. Chem.* **1991**, *30*, 65.

(2) Mui, H. D.; Poli, R. *Inorg. Chem.* **1989**, *28*, 3609.

0002-7863/92/1514-6723$03.00/0

electrons in a $\sigma^2\pi^2\delta^{*2}$ ground state. The two compounds have a completely identical molecular geometry (except for the metal–metal separation), as illustrated in I.

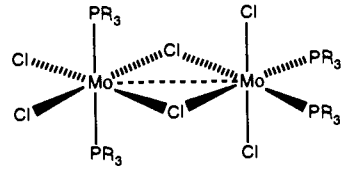

I

For the dimer without the metal–metal bond, the phosphine α protons can be observed in the ^{1}H NMR at ca. −30 δ at room temperature, a region typical of the same protons in mononuclear (S = 3/2) Mo(III) complexes, and their temperature dependence is consistent with a Curie behavior.[1] For the metal–metal bonded dimer, on the other hand, the phosphine α protons resonate at ca. 1 δ in the ^{1}H NMR at room temperature, and the decrease of paramagnetic shift with a decrease of temperature is consistent with the slight population of one or more paramagnetic excited states.

As previously discussed,[1,3] this dichotomy can be rationalized with the existence of two competing stabilization energies starting from the ideal situation of two noninteracting, "monoelectronic" t_{2g}^3 (in ideal octahedral symmetry) configurations. One stabilization is related to the metal–metal bonding overlap between the two pseudo-t_{2g} sets, and it stabilizes the metal–metal bonded structure. The other stabilization has to do with electronic correlation, as expressed by the familiar coulombic and exchange interactions, and it leads to a more stable nonbonded structure with three unpaired electrons per metal atom. For a mononuclear complex with a t_{2g}^3 configuration in an ideal O_h symmetry, the ground state will be of type $^4A_{2g}$. Thus, the ground state for a nonbonded edge-sharing bioctahedral compound results from the combination of the two $^4A_{2g}$ states from each half of the molecule, to give a manifold of states of B_{1u} type in ideal D_{2h} symmetry. Obviously, these two stabilization factors are delicately balanced in edge-sharing bioctahedral Mo(III) dimers, whereas stronger preferences are observed for the metal–metal bonded structure in the tungsten analogue, $W_2Cl_6(PEt_3)_4$,[4] and for the nonbonded structure in the chromium analogue, $Cr_2Cl_6(PEt_3)_4$.[5]

We were interested in further exploring the influence of the phosphine substituents on the ability of the two Mo(III) centers to bind to each other. According to the above model, the substituents may be expected to have an electronic effect on the strength of the metal–metal $\sigma^2\pi^2\delta^{*2}$ bond and/or on the stabilization of the pseudo-$^4A_{2g}$ configuration around each metal center and, in addition, a steric effect might be present. It does not seem likely that the most important effect is an electronic control on the metal–metal overlap, because that being the case a stronger bond would be expected for the compound with the electronically more releasing phosphine (PEt_3), contrary to what is observed. An electronic control on the stabilization of the high-spin, nonbonded structure can only be evaluated based on the knowledge of the nephelauxetic parameters for the various phosphine ligands, which have not been determined to the best of our knowledge. In absences of these parameters, we have decided to gather more experimental data by changing the nature of the phosphine substituents in a more rational and systematic fashion.

We report here the formation and solution characterization by ^{1}H NMR of new edge-sharing bioctahedral derivatives with either a set of four identical phosphine ligands, $Mo_2Cl_6L_4$, or with a mixed ligand set, $Mo_2Cl_6L_3L'$ and $Mo_2Cl_6L_2L'_2$, which were primarily obtained by reaction of face-sharing bioctahedral (FSBO) complexes of Mo(III), $Mo_2Cl_6L_3$, with a phosphine L or L′. These investigations also help in elucidating the mechanism of the FSBO-to-ESBO transformation.

Experimental Section

All operations were carried out under an atmosphere of prepurified dinitrogen by using standard glovebox and Schlenk line techniques. Solvents were purified by conventional methods and distilled under dinitrogen prior to use. The NMR spectra were recorded on a Bruker WP200 instrument in thin-walled 5-mm o.d. tubes. UV/visible spectra were recorded on a Milton Roy Spectronic 3000 Array spectrophotometer with IBM Software. The elemental analyses were by M–H–W, Phoenix, Arizona. $MoCl_3(THF)_3$,[6] $Mo_2Cl_6(PEt_3)_3$,[1] and $Mo_2Cl_6(PEt_3)_4$[2] were prepared by the described literature procedures. PMe_2Et and $PMeEt_2$ were prepared by standard methodologies[7] from PMe_2Cl and PEt_2Cl, respectively, and MeMgBr or EtMgBr in the proper stoichiometric ratio.[8] PMe_3 was purchased from Aldrich and trap-to-trap distilled prior to use. PMe_3-d_9 was prepared according the procedure reported by Wengel and Bergman.[9]

Preparation of $Mo_2Cl_6L_3$. (a) L = PMe_3. $MoCl_3(THF)_3$ (925 mg, 2.21 mmol) was placed in a Schlenk flask equipped with a magnetic stirrer bar and reflux condenser. Toluene (10 mL) was added, yielding a red suspension, followed by PMe_3 (380 μL, 3.67 mmol). The mixture was warmed to reflux, during which time the solid went up into solution. After 25 min, the solution was a deep purple color, and a dark colored solid was seen on the side walls of the Schlenk. Cooling to room temperature, followed by filtration, afforded a purple solid that was washed with 3 × 5 mL aliquots of heptanes and pumped to dryness. Recrystallization from CH_2Cl_2/heptanes yielded pure $Mo_2Cl_6(PMe_3)_3$ (380 mg, 64%). Anal. Calcd for $C_9H_{27}Cl_6Mo_2P_3$: C, 17.08; H, 4.30. Found: C, 16.83; H, 4.49. The ^{1}H NMR of this compound is presented in the Results section.

(b) L = PMe_2Et. $MoCl_3(THF)_3$ (111 mg, 0.26 mmol) was placed in a Schlenk flask equipped with a magnetic stirrer bar and reflux condenser. Toluene (5 mL) was added followed by PMe_2Et (47 μL, 0.40 mmol assuming a density of 0.76 g/mL).[10] The mixture was warmed to reflux, leading to darkening of the solution. Overnight reflux led to the formation of a purple/black solution and minor amounts of an insoluble material. After cooling to room temperature and filtration, the solution was layered with heptanes (12 mL). When diffusion of the two layers was complete, dark crystalline $Mo_2Cl_6(PMe_2Et)_3$ was isolated by removal of the mother liquor, washing with heptanes and pumping to dryness under vacuum: yield 51 mg (57%). Anal. Calcd for $C_{12}H_{33}Cl_6Mo_2P_3$: C, 21.36; H, 4.93. Found: C, 21.41; H, 4.93. The ^{1}H NMR of the freshly dissolved compound ($CDCl_3$, room temperature) is consistent with it being mainly present as the anti isomer (expected 6:6:6 for Me, 2:2:2 for Et(CH_2), and 6:3 for Et(CH_3)). Found (δ): 1.91 (6 H), 1.53 (3 H), −0.11 (6 H), −0.18 (6 H), −0.75 (6 H). In addition, there were several other minor peaks in the 2.1–0.0 region, some of which are presumably due to minor impurities and/or to minor proportions of the gauche isomer, but some may be attributed to the methylene protons of the anti isomer.

(c) L = $PMeEt_2$. This compound was prepared in an identical manner to $Mo_2Cl_6(PMe_2Et)_3$ (see above), using 287 mg of $MoCl_3(THF)_3$ (0.68 mmol), 10 mL of toluene, and 132 μL of $PMeEt_2$ (0.99 mmol assuming a density of 0.78 g/mL):[10] yield 120 mg (49%). Anal. Calcd for $C_{15}H_{39}Cl_6Mo_2P_3$: C, 25.13; H, 5.48. Found: C, 24.51; H, 5.80. The ^{1}H NMR of the freshly dissolved compound ($CDCl_3$, room temperature) is consistent with it being mainly present as the anti isomer (expected 6:3 for Me, 2:2:2:2:2:2 for Et(CH_2), and 6:6:6 for Et(CH_3)). Found (δ): 2.32 (6 H), 2.0 (6 H), 1.7–1.2 (big singlet with shoulders, total intensity ≈ 18 H, probably containing a resonance of Et(CH_3) for 6 H and all the methylene proton resonances), −0.30 (6 H), and −1.04 (3 H). As for the analogous PMe_2Et complex described above, there were other minor peaks that could be attributed to minor impurities and/or to minor proportions of the gauche isomer.

Preparation of $Mo_2Cl_6(PMe_3)_4$. $Mo_2Cl_6(PMe_3)_3$ (362 mg, 0.57 mmol) was placed in a Schlenk tube together with a stirring bar, and CH_2Cl_2 (10 mL) was added to produce a deep purple solution. PMe_3 (65 μL, 0.65 mmol) was injected into the solution via a microsyringe. After stirring for 2 min at room temperature, the solution was layered with an

(3) Poli, R. *Comments Inorg. Chem.* **1992**, *12*, 285.
(4) Chacon, S. T.; Chisholm, M. H.; Streib, W. E.; Van Der Sluys, W. *Inorg. Chem.* **1989**, *28*, 5.
(5) Cotton, F. A.; Eglin, J. L.; Luck, R. L.; Son, K. *Inorg. Chem.* **1990**, *29*, 1802.
(6) Poli, R.; Gordon, J. C. *Inorg. Chem.* **1991**, *30*, 4550.
(7) Henderson, W. A.; Buckler, S. A. *J. Am. Chem. Soc.* **1960**, *82*, 5794.
(8) PMe_2Et: ^{1}H NMR (C_6D_6, δ) 1.17–0.85 (m, 5 H, Et), 0.79 (d, 6 H, 2 Me, J_{PH} = 2.7 Hz); $^{31}P\{^1H\}$ NMR (C_6D_6, δ) −48.4. $PMeEt_2$: ^{1}H NMR (C_6D_6, δ) 1.3–0.85 (m, 10 H, 2 Et), 0.78 (d, 3 H, Me, J_{PH} = 1.7 Hz); $^{31}P\{^1H\}$ NMR (C_6D_6, δ) −34.0.
(9) Wenzel, T. T.; Bergman, R. G. *J. Am. Chem. Soc.* **1986**, *108*, 4856.
(10) The density of the mixed phosphine compounds PMe_2Et and $PMeEt_2$ are calculated by interpolation from the known densities of PMe_3 (d = 0.735 g/mL) and PEt_3 (d = 0.800 g/mL): Aldrich Catalog of Fine Chemicals, 1988–1989.

equal volume of heptanes, and the tube was carefully transferred to a −20 °C freezer where diffusion of the layers was allowed to occur. When diffusion was complete, a mixture of dark microcrystalline powder and larger crystals was separated by decanting off the mother liquor, followed by drying under vacuum: yield 50 mg. Upon microscopic inspection, the dark crystalline material looked purplish, and very minor quantities of a yellow-orange material were also observed. ^1H NMR spectroscopy showed that the material consists mainly of $Mo_2Cl_6(PMe_3)_4$ (see Results) containing minor amounts of other diamagnetic materials, but no peaks due to paramagnetic $MoCl_3(PMe_3)_3$ could be detected. Anal. Calcd for $C_{12}H_{36}Cl_6Mo_2P_4$: C, 20.33; H, 5.12. Found: C, 20.17; H, 4.94.

Attempted Preparation of $Mo_2Cl_6(PMeEt_2)_4$. $MoCl_3(THF)_3$ (360 mg, 0.86 mmol) was placed in a Schlenk flask equipped with a magnetic stirrer bar. THF (5 mL) was added followed by $PMeEt_2$ (230 μL, 1.72 mmol). The mixture was allowed to react for 2 h, giving a yellow solution. At this time the solution was evaporated to dryness. Toluene (5 mL) was added to the residue, and the mixture was brought to reflux for 10 min, during which time the solution turned dark. After removal of a minor amount of insoluble material, the solution was layered with heptanes (ca. 5 mL) and placed at −20 °C for diffusion to occur. The dark solid that formed was isolated by decanting off the mother liquor, washing with heptanes, and drying in vacuo. ^1H NMR spectroscopy revealed that the solid was a mixture of $Mo_2Cl_6(PMeEt_2)_3$ and $Mo_2Cl_6(PMeEt_2)_4$, with the FSBO dimer being the predominant species.

^1H NMR Investigation of the Interaction Between $Mo_2Cl_6L_3$ and L′ (L, L′ = PMe_3, PMe_2Et, $PMeEt_2$, PEt_3). All these reactions were conducted in a similar manner. A detailed description is given for the particular case where L = PMe_3 and L′ = PEt_3. $Mo_2Cl_6(PMe_3)_3$ (16 mg, 0.025 mmol) was dissolved in ca. 1 mL of $CDCl_3$, and the resulting solution was transferred via cannula into a thin-walled 5-mm o.d. NMR tube equipped with a rubber septum. After cooling to the dry ice temperature, PEt_3 (7.5 μL, 0.051 mmol) was injected into the solution, and the tube kept at −78 °C until the introduction into the NMR probe.

Preparation of $[PPN][Mo_2Cl_7(PMe_3)_2]$. $MoCl_3(THF)_3$ (878 mg, 2.10 mmol) was dissolved in 15 mL of CH_2Cl_2 and stirred for ca. 2 h at room temperature to complete its conversion to $Mo_2Cl_6(THF)_3$.[11] To the resulting purple solution were added PMe_3 (217 μL, 2.09 mmol) and PPN^+Cl^- (606 mg, 1.06 mmol). Stirring was continued overnight, to result in the precipitation of the product, which was filtered off, washed with heptane (2 × 10 mL), and dried in vacuo: yield 241 mg (25%). The ^1H NMR spectrum of this material in CD_2Cl_2 shows resonances at δ −0.69 and −0.86 for the syn and gauche isomers, in close correspondence with those reported for the analogous $PHMe_3^+$ salt.[12]

Results

Reaction Strategies. The preparation of the FSBO starting materials is standard and follows the procedure already reported by us for the preparation of the analogous $Mo_2X_6L_3$ (X = Cl, L = PEt_3, PMe_2Ph;[1] X = Br, I, L = PMe_2Ph[13]) derivatives (see eq 1).

$$2MoCl_3(THF)_3 + 3L \rightarrow Mo_2Cl_6L_3 + 6THF \quad (1)$$

These materials can be converted to the corresponding ESBO complexes by further interaction with 1 equiv of phosphine, which is the same strategy that has previously been reported for the preparation of $Mo_2Cl_6(PMe_2Ph)_4$.[1] This procedure has also been used to generate mixed-phosphine systems (eq 2).

$$Mo_2Cl_6L_3 + L' \rightarrow Mo_2Cl_6L_3L' \quad (2)$$

From the point of view of product isolation, this procedure has proven successful only for the tetrakis-PMe_3 complex, $Mo_2Cl_6(PMe_3)_4$. In the other cases (tetrakis-PMe_2Et or $PMeEt_2$ complexes and all the mixed phosphine systems) the compounds have only been characterized in solution by ^1H NMR, since these materials form in admixture with other byproducts (see below), and attempts to isolate them out of solution always give oily impure products. The tetrakis-$PMeEt_2$ compound does not form in significant amounts under the above conditions. Solutions of this compound were generated following the procedure reported for the preparation of $Mo_2Cl_6(PEt_3)_4$,[2] that is interaction between $MoCl_3(THF)_3$ with 2 equiv of $PMeEt_2$ in THF followed by brief reflux in toluene. Even in this case, however, a mixture of compounds (the desired ESBO product and the corresponding FSBO compound, the latter being predominant) was obtained.

The reason for the formation of byproducts is related to the thermodynamic instability of the ESBO $Mo_2Cl_6L_4$ compounds toward ligand disproportionation[1] as illustrated in eq 3, see also Discussion.

$$3Mo_2Cl_6L_4 \rightarrow 2Mo_2Cl_6L_3 + 2MoCl_3L_3 \quad (3)$$

The FSBO anionic complex $[Mo_2Cl_7(PMe_3)_2]^-$ has been reported earlier as the $PHMe_3^+$ salt and was obtained from the interaction of $Mo_2Cl_4(PMe_3)_4$ and Cl_2, a reaction that was intended to produce a different compound, namely $Mo_2Cl_6(PMe_3)_4$.[12] We have found a more logical route to this complex, as shown in eq 4, which parallels the route reported earlier for the preparation of salts of the $[Mo_2I_7(PMe_3)_2]^-$ ion.[14]

$$2MoCl_3(THF)_3 + 2PMe_3 + PPNCl \rightarrow PPN[Mo_2Cl_7(PMe_3)_2] + 6THF \quad (4)$$

Face-Sharing Bioctahedral Complexes, Anti–Gauche Isomerism. All FSBO complexes of type $Mo_2X_6L_3$ (X = halogen; L = monodentate phosphine) reported so far have been shown to be present in solution as mixtures of the two possible isomers, anti **II** and gauche **III**.[1,13] In the solid state, however, only the anti isomer has been identified so far. This situation is similar to that reported for the FSBO $[Mo_2X_7(PMe_3)_2]^-$ (X = Cl, I)[12,14] which can exist as syn and gauche isomers in solution. For X = Cl, both isomers have been obtained in the solid state.[12]

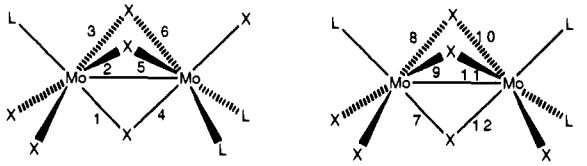

II III

When fresh solutions of $Mo_2Cl_6(PMe_3)_3$ are investigated by ^1H NMR in $CDCl_3$, two major peaks in a 2:1 ratio are observed at δ 0.04 and −0.55 (in $CDCl_3$) or at δ −0.02 and −0.63 (acetone-d_6). Other minor peaks are also present: these are assigned to the gauche isomer (see Figure 1). We have attempted to investigate the equilibrium between anti and gauche isomers of $Mo_2Cl_6(PMe_3)_3$ in $CDCl_3$ and in acetone-d_6. Unfortunately, decomposition reactions occur in each solvent, with the production of the known $[Mo_2Cl_7(PMe_3)_2]^-$ complex (syn and gauche mixture: peaks at δ −0.61 and −0.71 in $CDCl_3$,[12] −1.05 and −1.16 in acetone-d_6). This material results by replacement of a PMe_3 ligand in $Mo_2Cl_6(PMe_3)_3$ with Cl^-, the latter being presumably produced in $CDCl_3$ by reaction of PMe_3 with the solvent, and in acetone-d_6 by ionic dissociation equilibria. In the $CDCl_3$ reaction, the neutral $Mo_2Cl_6(PMe_3)_3$ compound is eventually completely consumed (several days at 30 °C) and additional as yet unidentified products are also formed. At no time during the monitoring of this reaction do we see the accumulation of the peaks that can be assigned to the gauche isomer to more than a few percent. In the acetone-d_6 reaction, monitoring for 24 h at room temperature shows the relatively fast growth of peaks that can be assigned to *gauche*-$Mo_2Cl_6(PMe_3)_3$, which level off to ≤20% of the total concentration for this compound (Figure 1c). For this complex, three signals in a 1:1:1 ratio are expected. Two resonances are evident at δ −0.48 and −0.58. The third peak could be the one observed in Figure 1b at δ −1.06, which accidentally overlaps with the resonance developing later (Figure 1c) for *syn*-$[Mo_2Cl_7(PMe_3)_2]^-$, but it is also possible that the third missing peak may be hidden underneath the stronger resonance at δ −0.02 for the anti isomer, in which case the spectra would indicate the selective formation of *syn*-$[Mo_2Cl_7(PMe_3)_2]^-$ (peak at δ −1.06 in Figure 1b) preceding its equilibration with the gauche isomer (peak at δ −1.16 in Figure 1c; equilibrium of syn/gauche ≈ 1:2[12]). The conclusions that

(11) Poli, R.; Mui, H. D. *J. Am. Chem. Soc.* **1990**, *112*, 2446.
(12) Cotton, F. A.; Luck, R. L. *Inorg. Chem.* **1989**, *28*, 182.
(13) Ahmed, K. J.; Gordon, J. C.; Mui, H. D.; Poli, R. *Polyhedron* **1991**, *10*, 1667.
(14) Cotton, F. A.; Poli, R. *Inorg. Chem.* **1987**, *26*, 3310.

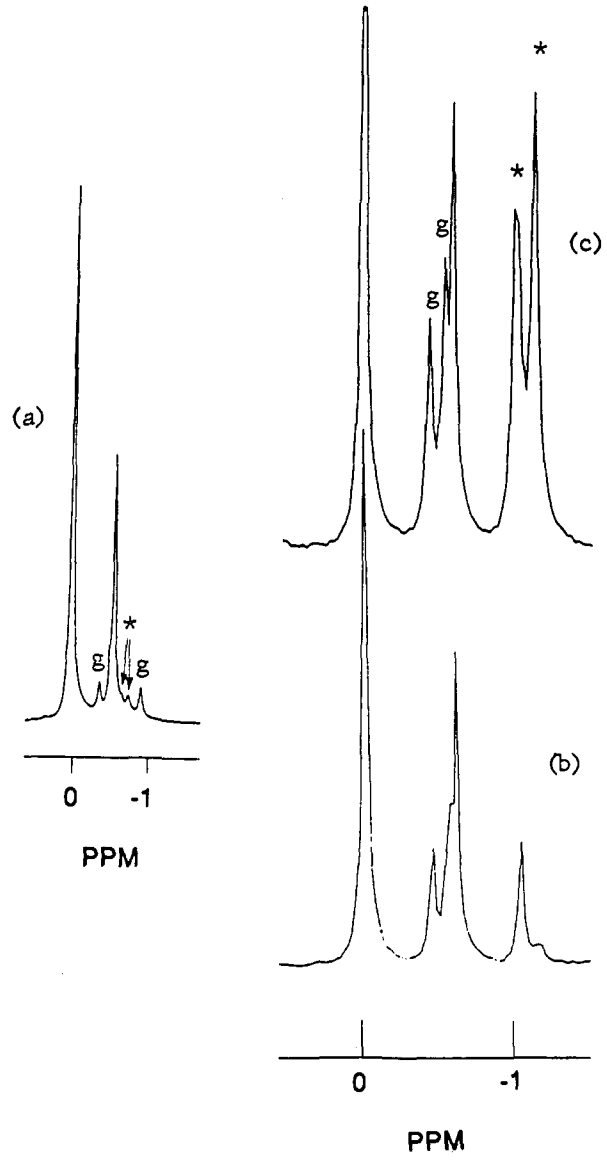

Figure 1. ^{1}H NMR spectra of solutions of $Mo_2Cl_6(PMe_3)_3$: (a) in $CDCl_3$, recorded immediately; (b) in acetone-d_6, recorded after 8 min at room temperature; (c) in acetone-d_6, recorded after 24 h at room temperature. Legend: g, peak assigned to the gauche isomer; *, peaks due to *syn*- and *gauche*-$[Mo_2Cl_7(PMe_3)_2]^-$ complex.

emerge from these investigations are that (i) the equilibration of the two possible isomers for the neutral $Mo_2Cl_6(PMe_3)_3$ complex is faster than for the charged $[Mo_2Cl_7(PMe_3)_2]^-$ complex[12] and (ii) a relatively higher proportion of gauche isomer is obtained in the acetone solvent with respect to $CDCl_3$, but the system does not reach the statistical equilibrium observed for syn and gauche isomers of the $[Mo_2Cl_7(PMe_3)_2]^-$ anion, indicating a slight thermodynamic preference for the anti isomer in the neutral system.

Analogous isomerization studies were not carried out on the FSBO derivatives containing unsymmetrical phosphines, i.e., $Mo_2Cl_6(PMe_2Et)_3$ and $Mo_2Cl_6(PMeEt_2)_3$, given the lower symmetry which results in much more complex spectral changes. However, the ^{1}H NMR spectra obtained on fresh solutions are again consistent with these materials having prevalently an anti configuration (see Experimental Section). It is worth noting that the most upfield shifted resonances (due to the phosphine α-protons) are more upfield shifted the greater number of ethyl groups vs methyl groups are present as phosphine substituents.

Generation and ^{1}H NMR Spectra of Homoleptic Phosphine Edge-Sharing Bioctahedral Derivatives, $Mo_2Cl_6(PMe_xEt_{3-x})_4$. The formation of $Mo_2Cl_6(PMe_3)_4$ from $Mo_2Cl_6(PMe_3)_3$ and PMe_3 has been monitored by ^{1}H NMR in acetone-d_6. This solvent was chosen because, as shown above, an observable proportion of the gauche isomer is present in this solvent, thus allowing us to address the possible different reactivity of the two FSBO dimers toward addition of phosphine. The important points are the following: (i) the reaction proceeds according to eq 5 in analogy with the corresponding PEt_3 and PMe_2Ph reactions and (ii) the rate of the first step is comparatively smaller than that of the second step in acetone-d_6 with respect to the corresponding reaction of the PMe_2Ph system in chlorinated hydrocarbons. In other words, the formation of mononuclear $MoCl_3(PMe_3)_3$ (resonances at δ −16.8 and −33.1) was noted before the FSBO compound was completely consumed. (iii) The gauche isomer was consumed *at the same rate* as the anti isomer. This fact is consistent either with two independent reactions for the two isomers that proceed at the same rate or with one of the two isomers reacting faster than the other one but nevertheless at a rate that is inferior to the isomerization rate. As observed in the preceding section, the anti/gauche isomerization rate appears to be relatively high. (iv) Approximately 50% of the starting material was consumed within 10 min at room temperature with production of significant amounts of monomer. Later, the reaction slowed down considerably due to the insufficient amount of free PMe_3 remaining in solution. (v) The final reaction mixture (ca. 24 h at room temperature) showed no residual ESBO dimer, consistent with the thermal instability of this material toward disproportionation (eq 3). The major components in the final spectrum are the monomer, the anti and gauche FSBO dimer, and the two isomers of the $[Mo_2Cl_7(PMe_3)_2]^-$ complex whose resonances remain approximately constant throughout the course of the reaction.

$$Mo_2Cl_6L_3 \xrightarrow{L} Mo_2Cl_6L_4 \xrightarrow{L} 2MoCl_3L_3 \qquad (5)$$

$Mo_2Cl_6(PMe_3)_4$ shows two peaks in a 1:1 ratio (at δ ca. −0.1 and −0.8 in $CDCl_3$, see Figure 2a, and at δ ca. −1.7 and −2.5 in acetone-d_6 at room temperature). This suggests that the structure is identical to those found for the analogous PEt_3 and PMe_2Ph compounds, that is two phosphine ligands are in axial positions on one metal center, while the other two are in equatorial positions on the other metal center (see **I**). However, the small paramagnetic shift indicates that *the two metals are bonded to each other* as is the case for the PMe_2Ph compound and unlike what was found for the PEt_3 compound.[1] The data also indicate a significant solvent effect on the paramagnetic shift of the proton signals.

Incidentally, a compound of formula $\{MoCl_3(PMe_3)_2\}$ has been reported before, which was obtained from prolonged reflux of $MoCl_3(PMe_3)_3$ in toluene.[15] This material was characterized only by elemental analysis, melting point, and low-energy IR. We do not think this material is identical to the ESBO $Mo_2Cl_6(PMe_3)_4$ compound reported here, because we find that the latter compound disproportionates according to eq 3 under the conditions in which $\{MoCl_3(PMe_3)_2\}$ was said to be obtained. Our attempts to reproduce this work resulted in the formation of $Mo_2Cl_4(PMe_3)_4$ (identified by comparison of the UV/vis spectrum with that reported[16] in the literature) and a white insoluble material, presumably $PMe_3H^+Cl^-$.[17]

The structure shown in **I** is consistent also with the ^{1}H NMR spectra obtained for the other ESBO derivatives with PMe_2Et and $PMeEt_2$. For the PMe_2Et derivative, structure **I** should give rise to a 12:12:4:4 pattern for the α-proton resonances (methyl group protons and methylene protons of the ethyl groups), whereas a 6:6:4:4:4:4 pattern is predicted for the same protons of the $PMeEt_2$ compound. The actual resonances in the α-proton region are shown in Figure 2 (parts b and c) and listed in Table I. Partial overlap of the peaks makes it impossible to assign each individual resonance. However, for the PMe_2Et compound (Figure 2b), the two groups of resonances integrate as 20:12, and the clear presence of at least three peaks rules out the most likely structural alter-

(15) Carmona, E.; Galindo, E.; Sanchez, L.; Nielson, A. J.; Wilkinson, G. *Polyhedron* **1984**, *3*, 347.
(16) Cotton, F. A.; Extine, M. W.; Felthouse, T. R.; Kolthammer, B. W. S.; Lay, D. G. *J. Am. Chem. Soc.* **1981**, *103*, 4040.

Table I. ^1H NMR Resonances for the ESBO $Mo_2Cl_6(PMe_xEt_{3-x})_4$ Complexes with Structure I[a]

compound	α protons [PMe_3/$PEt_3(CH_2)$]	PEt_3 (CH_3)	ref
$Mo_2Cl_6(PMe_3)_4$	−0.1, −0.8 (1:1)		this work
$Mo_2Cl_6(PMe_2Et)_4$	−4.2 with sh at −4.5, −5.3 (20:12)	3.15, 2.26 (6:6)	this work
$Mo_2Cl_6(PMeEt_2)_4$	−18, −21.5, −23, −24, −25 (ca. 6:4:10:4:4)	8.8, 6.2 (12:12)	this work
$Mo_2Cl_6(PEt_3)_4$	−28.7 (4)	9.9, 7.8 (3:3)	1

[a] Solv = $CDCl_3$ or CD_2Cl_2. Temperature = 293 ± 2 K.

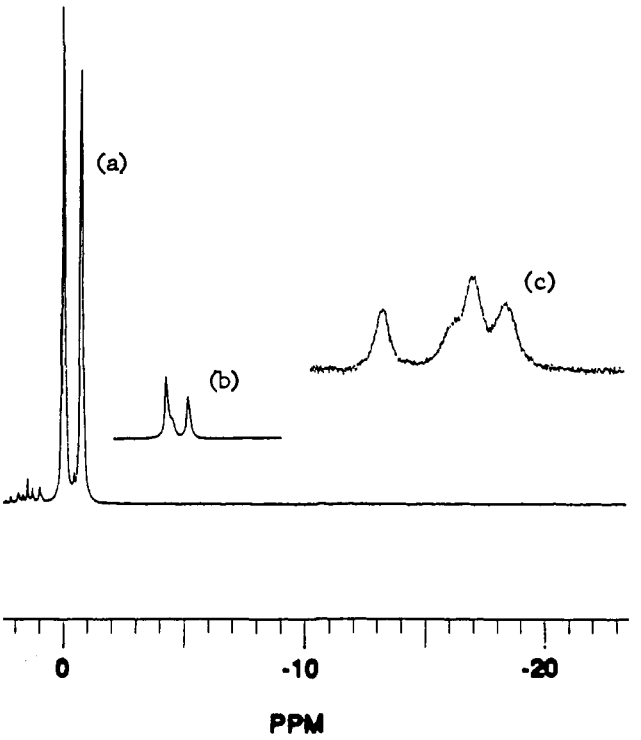

Figure 2. ^1H NMR spectra ($CDCl_3$) in the phosphine α-proton region: (a) $Mo_2Cl_6(PMe_3)_4$, room temperature; (b) $Mo_2Cl_6(PMe_2Et)_4$, room temperature; (c) $Mo_2Cl_6(PMeEt_2)_4$, T = 240 K.

natives with all four phosphine ligands in equatorial positions [analogous to $Zr_2Cl_6(PR_3)_4$ (R = Et, Bu) and $Hf_2Cl_6(PMe_2Ph)_4$][18] or with all four phosphine ligands in axial positions. In those cases, only two peaks in a relative 24:8 ratio should have been present in the phosphine α-proton region for the PMe_2Et compound. The same can be said about the $PMeEt_2$ complex, for which the alternative all-equatorial structure would predict only three resonances in a 12:8:8 ratio. It is quite unlikely that the observed NMR spectra of Figure 1 (parts b and c) reflect the presence of a mixture of isomers. The methyl protons of the ethyl groups for these two $Mo_2Cl_6(PMe_xEt_{3-x})_4$ (x = 1, 2) compounds could also be identified and are consistent with the assignment of structure I to the ESBO product in each case (see Table I).

To be noted in Figure 2 and Table I is the progressive increase of the paramagnetic shift for the phosphine proton resonances as the ethyl substitution increases. These shifts are temperature dependent, and the average chemical shifts for the phosphine α proton resonances as a function of temperature in the four compounds are reported in Figure 3. The PMe_3 derivative shows only a slight increase of the paramagnetic shift as temperature increases, consistent with a diamagnetic ground state and a slightly populated paramagnetic (presumably a triplet $\delta^*\delta$)[1] excited state. The PMe_2Et derivative behaves similarly to the PMe_3 analogue, except that the paramagnetic shift is slightly greater. This can be rationalized by either a smaller $\delta^*-\delta$ gap, resulting in a more populated excited state, or by a higher population of a nonbonded isomer which is in rapid equilibrium with the bonded form (see Discussion). The observed shifts for the $PMeEt_2$ compound are most interesting. In this case, the average paramagnetic shift at

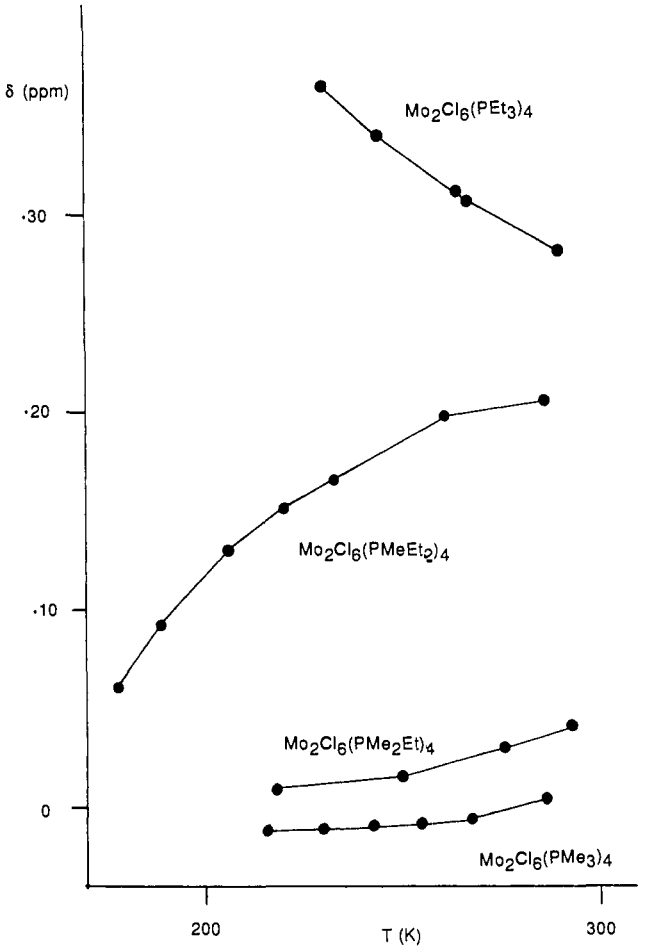

Figure 3. Average chemical shift as a function of temperature for the phosphine α-proton resonances in compounds $Mo_2Cl_6(PMe_xEt_{3-x})_4$ (x = 0–3).

room temperature is closer to that of the nonbonded PEt_3 complex. However, lowering the temperature induces a dramatic decrease of the shifts until at 178 K the average shift is much closer to those of the PMe_3 and PMe_2Et systems which presumably have a Mo–Mo bond. There is no evidence for freezing out of an equilibrium between two different isomers at 178 K. Finally, the behavior of the PEt_3 compound indicates at most a small antiferromagnetic coupling between two nonbonded, paramagnetic Mo(III) centers as discussed before.[1]

^1H NMR Monitoring of the Formation of Mixed-Phosphine Edge-Sharing Bioctahedral Derivatives. Besides reacting each $Mo_2Cl_6(PMe_xEt_{3-x})_3$ FSBO complex with an additional equivalent of the same PMe_xEt_{3-x} phosphine (phosphine "x"), we have also carried out a selected number of reactions with a different phosphine PMe_yEt_{3-y} (phosphine "y"), with the intention of generating mixed-phosphine $Mo_2Cl_6(PMe_xEt_{3-x})_3(PMe_yEt_{3-y})$ ESBO derivatives. The are two main reasons for carrying out these investigations. One reason is to see whether the attack by the incoming phosphine is selective. In fact, two different isomers can be obtained for the mixed phosphine product, one with phosphine y in an axial position and the other with the same phosphine in an equatorial position. It is also to be noted that different compounds can be made with the same number of methyl and ethyl groups by judicious choice of the starting materials, for instance a compound with nine methyl groups and three ethyl groups can be made either from $Mo_2Cl_6(PMe_3)_3$ + PEt_3 or from $Mo_2Cl_6(PMe_2Et)_3$ and PMe_3. If there is a preferred position of attack, we can use the above strategy to introduce particular substituents in particular desired positions. Thus, the second reason for carrying out these studies is to probe for the importance of the position of binding (axial vs equatorial) on the transmission of steric and electronic effects and ultimately on the ability of the

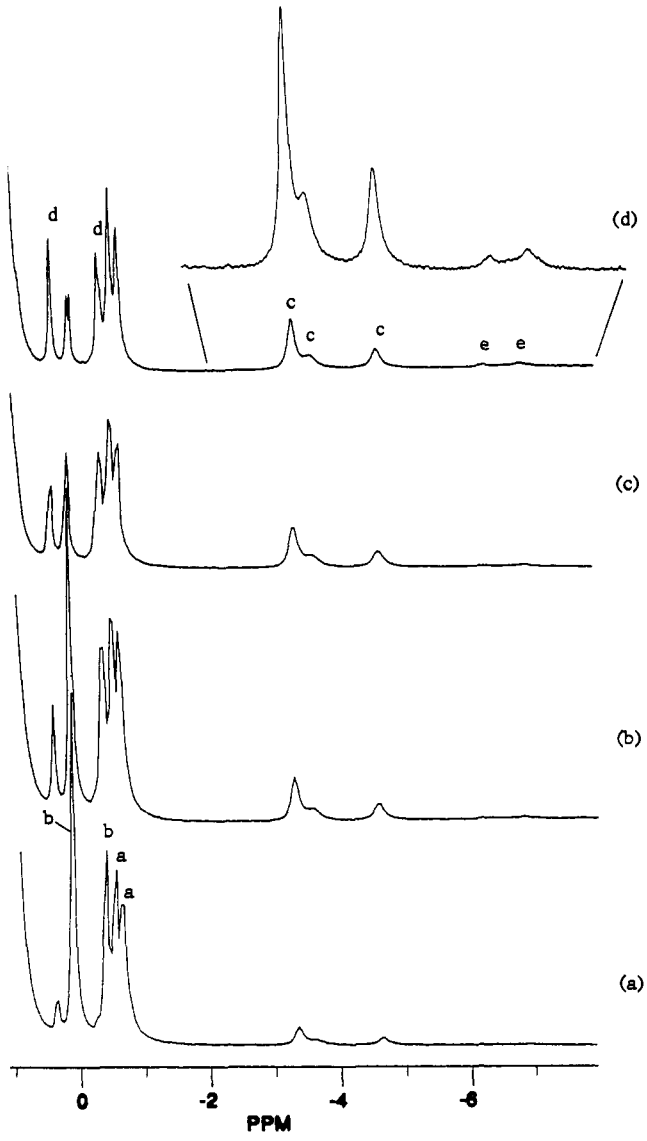

Figure 4. ^1H NMR monitoring of the reaction between $Mo_2Cl_6(PMe_3)_3$ and PEt_3 (solvent = $CDCl_3$, room temperature): (a) t = 5; (b); t = 13; (c) t = 30; (d) t = 45 min.

metals to establish a bonding interaction with each other.

We have run all these reactions in $CDCl_3$. In spite of the problems associated with this solvent when using reactive trialkylphosphines, e.g., formation of $[Mo_2Cl_7L_2]^-$ anions (see above), useful information was obtained because of the characteristic resonance region for the α-protons of the neutral ESBO products. The principal reason for choosing $CDCl_3$ over acetone-d_6, however, is our observation of a *higher accumulation* of the ESBO $Mo_2Cl_6(PMe_3)_4$ system when conducting the $Mo_2Cl_6(PMe_3)_3/PMe_3$ reaction in $CDCl_3$ with respect to acetone-d_6, before the edge sharing compound starts to significantly disproportionate according to eq 3 (see above). Thus a higher accumulation of the desired ESBO materials was reasonably expected also for the analogous reactions leading to mixed phosphine derivatives.

(i) **Reaction between $Mo_2Cl_6(PMe_3)_3$ and PEt_3.** This investigation gave us the maximum amount of information given the high symmetry of the starting complexes and products. The starting solution of the $Mo_2Cl_6(PMe_3)_3$ complex is impure by a mixture of *syn*- and *gauche*-$[Mo_2Cl_7(PMe_3)_2]^-$ (resonances labeled a, see Figure 4), presumably formed while gently warming the starting material to facilitate its dissolution. This impurity, however, does not appear to affect the outcome of the reaction with PEt_3 as it remains practically unchanged throughout the course of the reaction. Furthermore, a control experiment carried out by adding PEt_3 to $[PPN][Mo_2Cl_7(PMe_3)_2]$ did not show the growth of any of the resonances illustrated in Figure 4.

Following the addition of PEt_3, the ^1H NMR spectrum changes as illustrated in Figure 4 (parts a–d). Only considerations relating to the resonances of phosphine α protons will be presented for this reaction and for the other ones described in this section. The resonances of the Et CH_3 protons in the ESBO products could not be assigned with certainty due to extensive overlap among the peaks of different products and starting materials and the low relative concentration levels achieved during the experiments. The relevant observations are the following: (i) the resonances due to *anti*-$Mo_2Cl_6(PMe_3)_3$ (labeled b) decrease and (ii) a set of new resonances in the δ −3 to −5 region (labeled c) appears first. These resonances can be assigned to the expected compound $Mo_2Cl_6(PMe_3)_3(PEt_3)$ (Me/Et ratio = 9:3). Three resonances are observed in this region (see Figure 4d); two of them partially overlap, but the areas of the sum of these two and the third peak are in an approximate ratio of 24:9. Whether the compound has an axial or an equatorial PEt_3 ligand cannot be established because three peaks in a 18:9:6 ratio are expected for either complex. This is true for any pair of phosphine ligands: structure **IV**, i.e., the one resulting from addition of the new phosphine L′ to the axial position, has a mirror plane passing through all four axial ligands, whereas structure **V**, i.e., the alternative structure with L′ occupying an equatorial position, has a mirror plane passing through all six (four terminal and two bridging) equatorial ligands. Therefore, both structures **IV** and **V** are expected to give the same *number and relative intensity* for all NMR resonances. However, we can conclude that *only one isomer* of the expected mixed phosphine ESBO product is present in solution, thus demonstrating the selective attack of PEt_3 at a specific position.

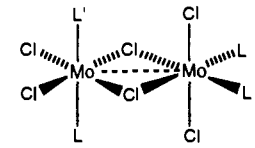

IV

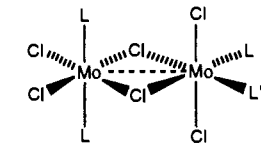

V

(iii) The paramagnetic shifts of the phosphine α-protons in the $Mo_2Cl_6(PMe_3)_3(PEt_3)$ product compare with those of the homoleptic PMe_2Et complex (Me/Et ratio = 8:4). (iv) At longer reaction times, new peaks in the α-proton region for the FSBO starting material (δ 0.5 to −1 region) that cannot be attributed to neither anti nor gauche tris-PMe_3 complex (labeled d) start to grow. Contemporarily, new peaks that are shifted further upfield from those of $Mo_2Cl_6(PMe_3)_3(PEt_3)$ (δ −6 to −7 region, labeled e in Figure 4) grow. After about 30 min from the start of the reaction, additional small peaks appear in the δ −30 to −50 region, attributed to mononuclear products of disproportionation (eq 3). (v) At much longer reaction times, the disproportionation reaction becomes predominant, rendering the ^1H NMR spectrum quite complex and devoid of useful information.

Although a more detailed discussion of the possible mechanism of this reaction will be presented in the Discussion section, we present a few considerations here as these will help to rationalize a few more results illustrated below. As discussed earlier in relation to the $Mo_2Cl_6(PMe_3)_3/PMe_3$ reaction, the anti and gauche FSBO isomers either accidentally react at the same rate with additional phosphine, or one of them is more reactive and the reaction is slow with respect to the isomer equilibration. As illustrated in Scheme I, the anti isomer has a simple pathway for the transformation into an ESBO product having the right stereochemistry if the incoming phosphine ligand attacks at the position trans to the unique phosphine, which should also be the most reactive position based on trans effect arguments.[6] This pathway requires a minimum of molecular rearrangement which is not paralleled in the analogous reaction of the gauche isomer. It would then seem logical to expect a higher reactivity for the anti isomer, which is the preponderant isomer in $CDCl_3$ solution. Under this assumption, we expect a *selective attack of the incoming phosphine at the axial position.* An analogous reaction investigated by Cotton[19] on the diamagnetic $Rh_2Br_6L_3$ + L′ system

Scheme I

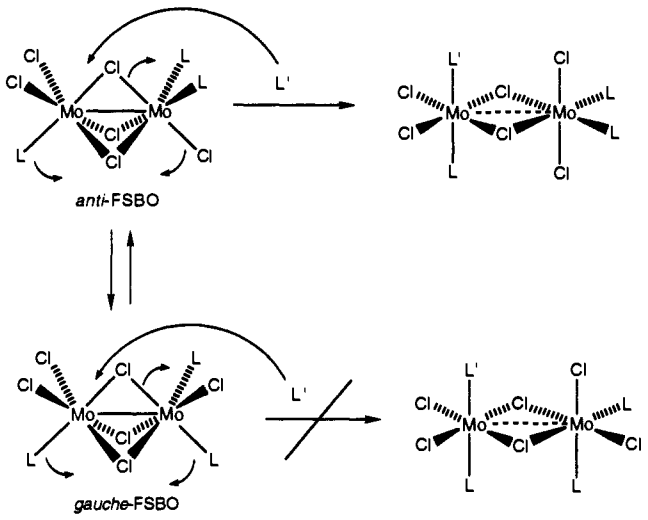

Scheme II

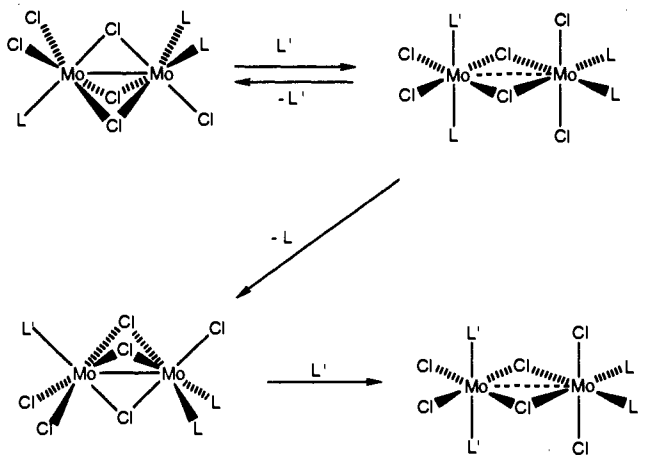

gives a firm indication of selective attack of L′ to the axial position: due to the characteristic pattern of ^{31}P–^{31}P and ^{31}P–^{103}Rh couplings for axial and equatorial phosphines in this system, the resulting $Rh_2Br_6L_3L'$ product is proven to have structure **I** and to contain the L′ ligand in an axial position. For the molybdenum compounds that are subject of the present study, the small paramagnetism makes it impossible to observe the ^{31}P resonances of coordinated phosphine ligands. For the remainder of this paper, we shall base all our considerations on the assumption that Scheme I is correct. Thus, we start by explicitly indicating the nature of the ESBO product as $Mo_2Cl_6(PMe_3)_3(ax\text{-}PEt_3)$.

We can now go further in the attempted rationalization of the experimental observations in Figure 4. Resonances d are in a region that is typical of FSBO materials,[1] whereas resonances e can only be attributed to a new ESBO product. In fact, all FSBO materials reported so far show relatively strong metal–metal interactions and the phosphine α proton resonances in the tri-μ-chloro systems are always downfield of δ −1, whereas mononuclear complexes always show resonances upfield of δ −17 for the same type of protons.[1,6] All peaks can be assigned according to a reactivity scheme that is based only on the higher trans effect of phosphines and on the reversibility of the *anti*-FSBO-to-ESBO transformation. As shown in Scheme II, the primary ESBO $Mo_2Cl_6L_3(ax\text{-}L')$ product can either dissociate L′ to reform the

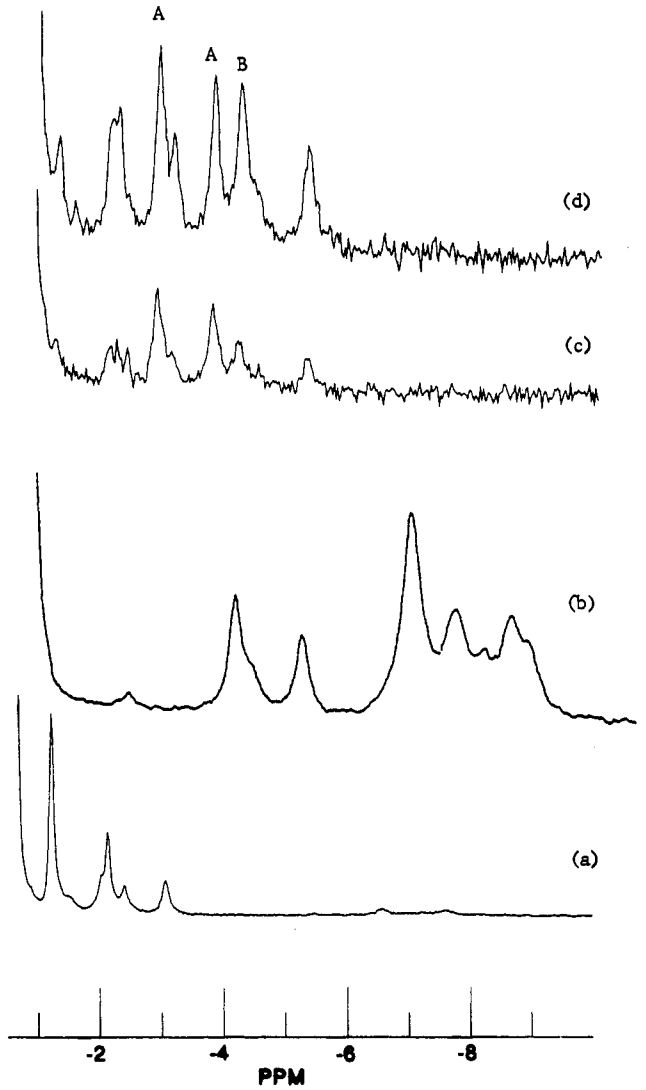

Figure 5. Selected portions of the ^1H NMR spectra of solutions obtained: (a) $Mo_2Cl_6(PMe_3)_3$ + $PMeEt_2$; (b) $Mo_2Cl_6(PMe_2Et)_3$ + $PMeEt_2$; (c) $Mo_2Cl_6(PMe_2Et)_3$ + PMe_3, after 20 min; (d) $Mo_2Cl_6(PMe_2Et)_3$ + PMe_3, after 100 min. All reactions were carried out at room temperature in $CDCl_3$.

starting FSBO complex, or the other axial ligand L can dissociate to form a *different* FSBO complex, i.e., *anti*-$Cl_2L'Mo(\mu\text{-}Cl)_3MoClL_2$. The relative rates of these two processes will depend upon the relative trans-labilizing ability of the two phosphine ligands L and L′. This new FSBO complex (L = PMe_3, L′ = PEt_3) can account for the new resonances labeled d in Figure 4. This new FSBO complex could then proceed by interacting with more L′ to form a new ESBO complex, $Mo_2Cl_6L_2(ax\text{-}L')_2$ having *both new phosphines L′ in mutually trans axial positions*. The resonances labeled e in Figure 4 can be assigned to the new ESBO complex $Mo_2Cl_6(PMe_3)_2(ax\text{-}PEt_3)_2$ (Me/Et ratio = 6:6). The pattern of the resonances is consistent with the expected two resonances in a 18:12 ratio for the assigned formula, and the higher paramagnetic shift with respect to resonances c is in accord with the higher number of ethyl groups with respect to the primary ESBO product, consistent with the trend observed for the homoleptic $Mo_2Cl_6(PMe_xEt_{3-x})_4$ complexes (see Figure 3). The same number and relative intensity of resonances is expected for the isomeric compound with both PMe_3 ligands in axial position and both PEt_3 ligands in equatorial position, whereas a less symmetrical substitution is predicted to give rise to more peaks.

(ii) Reactions between $Mo_2Cl_6(PMe_3)_3$ and $PMeEt_2$, between $Mo_2Cl_6(PMe_2Et)_3$ and $PMeEt_2$, and between $Mo_2Cl_6(PMe_2Et)_3$ and PMe_3. These reactions show general trends similar to those described above for the $Mo_2Cl_6(PMe_3)_3/PEt_3$ reaction. The

(17) Cotton, F. A.; Poli, R. *Inorg. Chem.* **1987**, *26*, 1514.

(18) (a) Wengrovius, J. H.; Schrock, R. R.; Day, C. S. *Inorg. Chem.* **1981**, *20*, 1844. (b) Cotton, F. A.; Diebold, M. P.; Kibala, P. A. *Inorg. Chem.* **1988**, *27*, 799. (c) Cotton, F. A.; Kibala, P. A.; Wojtczak, W. A. *Inorg. Chim. Acta* **1990**, *177*, 1.

(19) Cotton, F. A.; Eglin, J. L.; Kang, S.-J. *J. Am. Chem. Soc.* **1992**, *114*, 4015. We are grateful to Prof. Cotton for sharing with us his unpublished results and for helpful discussion.

relevant ^1H NMR spectra in the phosphine α-proton region for the ESBO products are shown in Figure 5. Noteworthy observations are the following: (a) for the product of the $Mo_2Cl_6(PMe_3)_3/PMeEt_2$ reaction (Figure 5a), the observed pattern (in the δ −1 to −3 range) is in close agreement with the expected five resonances in a 18:9:3:2:2 ratio for the ESBO product with three PMe_3 and one $PMeEt_2$ (Me/Et ratio = 10:2). On the basis of the previous discussion, we attribute these resonances to compound $Mo_2Cl_6(PMe_3)_3(ax\text{-}PMeEt_2)$. At longer reaction times, broader resonances appear in the δ −6 to −8 region, which may be attributed to a $Mo_2Cl_6(PMe_3)_2(ax\text{-}PMeEt_2)_2$ derivative (Me/Et ratio = 8:4), although the low concentration level achieved by this compound makes it impossible to argue as to their number and relative intensity. (b) For the $Mo_2Cl_6(PMe_2Et)_3/PMeEt_2$ reaction (Figure 5b), the expected pattern for the $Mo_2Cl_6(PMe_2Et)_3(ax\text{-}PMeEt_2)$ product (Me/Et ratio = 7:5) is nine peaks in a 6:6:6:3:2:2:2:2:2 ratio. The observed pattern is quite complex, consistent with a high number of inequivalent protons, but not much can be said about the number and relative intensity of the peaks. At longer times, we do not see buildup of additional resonances. Presumably, if any product of further phosphine substitution forms, that is $Mo_2Cl_6(PMe_2Et)_2(ax\text{-}PMeEt_2)_2$ (Me/Et ratio = 6:6), its α-proton resonances could end up in the same region as the primary ESBO product (δ −4 to −10), since the Me/Et substitution on the phosphine ligands in the two complexes is rather similar. (c) Finally, for the $Mo_2Cl_6(PMe_2Et)_3/PMe_3$ reaction (Figure 5 (parts c and d)), a comparison between the spectra taken at different times shows that at least two compounds are formed, one of which (peaks labeled A) precedes the formation of the other one (peak labeled B). The unlabeled resonances cannot be attributed to either species unambiguously. We attribute peaks A to the $Mo_2Cl_6(PMe_2Et)_3(ax\text{-}PMe_3)$ complex (Me/Et ratio 9:3), for which seven α-proton resonances in a 9:6:6:6:2:2:2 ratio are expected, and peak B to the $Mo_2Cl_6(PMe_2Et)_2(ax\text{-}PMe_3)_2$ compound (Me/Et ratio = 10:2) which should exhibit only three resonances in a 18:12:4 ratio. In this reaction, as proposed also for case (b) above, the ESBO product of further phosphine substitution has peaks in the same region as the primary product, the two compounds differing only by one Me vs Et substituent. However, in this case the secondary product is apparently forming at a higher rate with respect to any of the other cases discussed previously. A tentative rationalization of this phenomenon will be given in the Discussion section.

(iii) Reaction between $Mo_2Cl_6(PEt_3)_3$ and PMe_3 or PMe_3-d_9. The last reaction that we have investigated which results in the formation of a mixed phosphine ESBO product is the interaction between $Mo_2Cl_6(PEt_3)_3$ and PMe_3. This is a situation in which the primary product, $Mo_2Cl_6(PEt_3)_3(ax\text{-}PMe_3)$, has a high relative proportion of ethyl groups (Me/Et ratio = 3:9). As expected, the phosphine α-protons of the resulting ESBO products (see Figure 6a–c) are more upfield shifted with respect to those of the other ESBO materials with a higher Me/Et ratio described above. In this case, it appears that more products are formed at comparable rates as was also seen in the $Mo_2Cl_6(PMe_2Et)_3/PMe_3$ reaction described above. The primary ESBO product should have four peaks in a 9:6:6:6 ratio. There are more than four resonances among the one observed at δ −17 and those in the δ −25 to −28 range (Figure 6a–c). In addition, repetition of the same NMR experiment with different excess amounts of PMe_3 indicated that the peak at δ −17 had a different relative intensity with respect to the other resonances in different experiments (greater relative intensity for greater excess of PMe_3).

In order to gather more information on the nature of the observed resonances, we have carried out an analogous experiment where we used PMe_3-d_9 in place of PMe_3. The results are shown in Figure 6d–f. The resonances at δ −17 and −27.5 in Figure 6a–c can be straightforwardly assigned to PMe_3 resonances since these are absent in Figures 6d–f. Since only one PMe_3 resonance can be assigned to $Mo_2Cl_6(PEt_3)_3(ax\text{-}PMe_3)$, this experiment confirms that two PMe_3 containing products are being formed at a similar rate. The logical assumption, according to Scheme II, is that the second product is the symmetrically substituted $Mo_2Cl_6(PEt_3)_2(ax\text{-}PMe_3)_2$ (Me/Et ratio = 6:6). For this compound, two resonances in a 18:12 ratio are expected in analogy to the isomeric $Mo_2Cl_6(PMe_3)_2(ax\text{-}PEt_3)_2$ described above. The resonance at δ −17 is assigned to the PMe_3 ligands in this bis-PMe_3 ESBO product (relative intensity 18), whereas the corresponding PEt_3 methylene resonance (relative intensity 12) must be part of the δ −25 to −27 multiplet (cf. Figure 6 (parts a and d)). All resonances for the ESBO $Mo_2Cl_6(PEt_3)_3(ax\text{-}PMe_3)$ material are contained in the δ −25 to −27.5 region, with the PMe_3 resonance at δ −27.5. This assignment is also in line with smaller paramagnetic shifts expected (vide supra) for the more Me substituted ESBO product. The other resonances that become evident at longer reaction times (δ −19 in Figure 6c; δ −16.5, −18.5, −29.5, and −31.5 in Figure 6f; and other resonances further upfield shifted) may be attributed to mononuclear products and/or ESBO compounds having a different relative number and/or stereochemistry of PMe_3 and PEt_3 ligands.

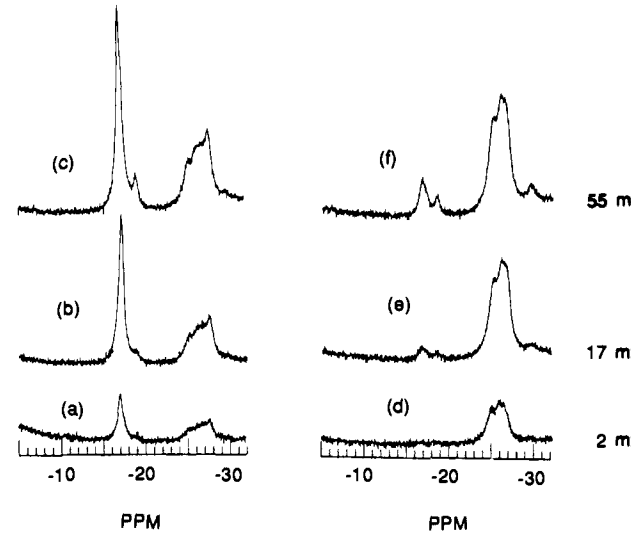

Figure 6. Time evolution of the ^1H NMR of solutions obtained from $Mo_2Cl_6(PEt_3)_3$ and (a)–(c), PMe_3; (d)–(f), PMe_3-d_9. The reactions were carried out at room temperature in $CDCl_3$.

A solution obtained independently by interacting $Mo_2Cl_6(PEt_3)_3$ and PMe_3 was subjected to a variable temperature ^1H NMR investigation. It was not possible, in the 221–293 K temperature range, to achieve a better resolution of the complex set of resonances observed between δ −25 and −27 at room temperature. The peaks assigned to the PMe_3 proton resonances for the two compounds, however, were discernible at all temperatures. The position of these peaks as a function of temperature is illustrated in Figure 7.

Discussion

Disproportionation of Edge-Sharing Bioctahedral Complexes. We have previously discovered[1] that the ESBO compounds $Mo_2Cl_6L_4$ with L = PEt_3 or PMe_2Ph are thermodynamically unstable toward the disproportionation reaction illustrated in eq 3. Although this reaction is relatively slow for the PEt_3 derivative, so that this compound can be generated by brief reflux of $MoCl_3(THF)_3$ and PEt_3 (2 equiv) in toluene,[2] the analogous reaction is faster for the PMe_2Ph derivative, and the compound cannot be prepared directly from $MoCl_3(THF)_3$ and PMe_2Ph.[1] However, we found that the reaction between FSBO $Mo_2Cl_6(PMe_2Ph)_3$ and PMe_2Ph occurs in two steps (see eq 5),[1] the first of which is much faster than the second, thus providing a kinetic strategy for the preparation of the ESBO complex. This has been our strategy in the synthesis of the $Mo_2Cl_6(PMe_3)_4$ compound. Unfortunately, for the more ethyl substituted [either homoleptic, e.g., $Mo_2Cl_6(PMe_2Et)_4$, or mixed-phosphine, e.g., $Mo_2Cl_6(PMe_3)_3(PEt_3)$] systems, two factors hampered the isolation of the desired products in a pure state. One factor is the decreased tendency to form crystalline solids for less symmetric systems, but perhaps the most important factor is a decrease of the relative rate of the first step

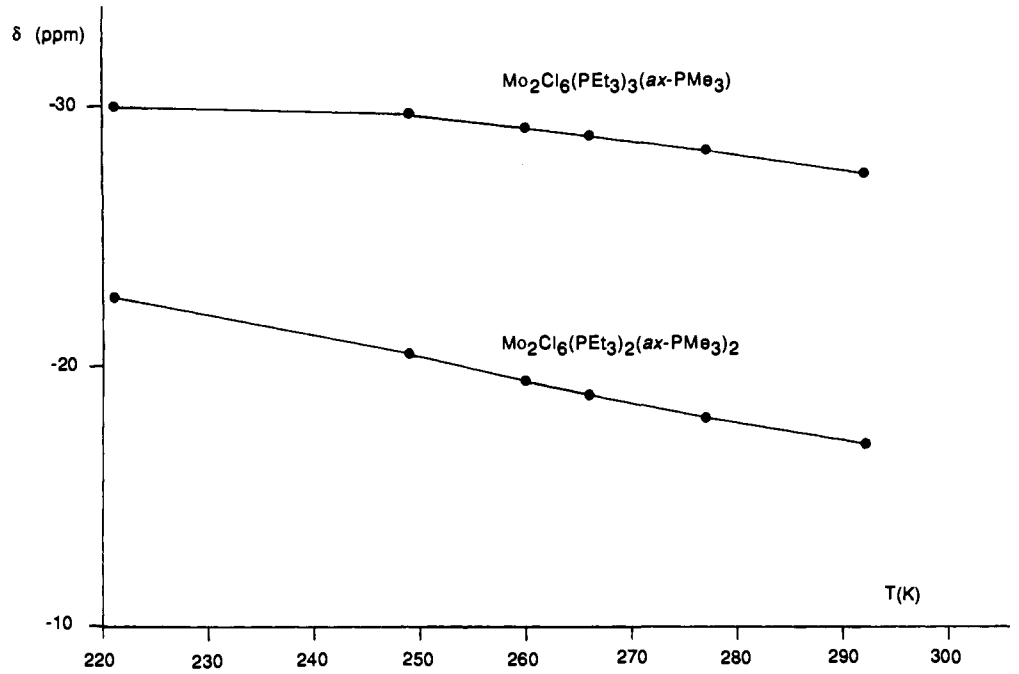

Figure 7. Chemical shift as a function of temperature for the PMe_3 α-proton resonances in compounds $Mo_2Cl_6(PEt_3)_3(PMe_3)$ and $Mo_2Cl_6(PEt_3)_2(PMe_3)_2$.

with respect to that of the second step in eq 5 as the number of ethyl groups increases. This is clearly shown by the ^1H NMR monitoring of the reactions between $Mo_2Cl_6L_3$ and L′ (which are faster when L and L′ are more methyl substituted phosphine), resulting in the formation of more complex mixtures of ESBO, FSBO, and mononuclear complexes as the Et/Me ratio increases.

Since the the disproportionation reaction presumably proceeds as illustrated in eqs 6a and 6b,[1] it is tempting to propose that the slow step is the one that has the highest component of metal–metal bond breaking (step 6a when the ESBO derivative is nonbonded, and step 6b when the ESBO derivative is bonded). This proposed scheme can rationalize the observed highest kinetic accumulation of the ESBO intemediate in eq 5 for the $Mo_2Cl_6L_4$ (L = PMe_3, PMe_2Ph) systems and the slowest disproportionation for *isolated* $Mo_2Cl_6(PEt_3)_4$.

$$Mo_2Cl_6L_4 \rightleftarrows Mo_2Cl_6L_3 + L \qquad (6a)$$

$$Mo_2Cl_6L_4 + 2L \rightarrow 2MoCl_3L_3 \qquad (6b)$$

Mechanism of Isomerization of Face-Sharing Bioctahedral Complexes and Transformation of Face-Sharing-to-Edge-Sharing Bioctahedral Complexes. In the Results we have presented arguments in support of the higher reactivity of anti vs gauche FSBO dimer and of the selective generation of an ESBO dimer where the incoming phosphine has taken up an axial position. In this section, we examine these topics and other related issues in more details.

First, we observe that there appears to be a thermodynamic preference for an ESBO ax,ax;eq,eq isomer. No other isomers have been observed structurally or by NMR for derivatives of Mo(III) as well as Cr(III), W(III), Ta(III), Ru(III), and Rh(III), with monodentate phosphine ligands.[4,5,20] The only exception to this rule (with no apparent explanation) is represented by d^1–d^1 ESBO dimers, which seem to prefer the all eq stereochemistry.[18,21] No evidence for ESBO complexes with a structure different than that illustrated in **I** has been obtained in the present study. Thus,

Scheme III

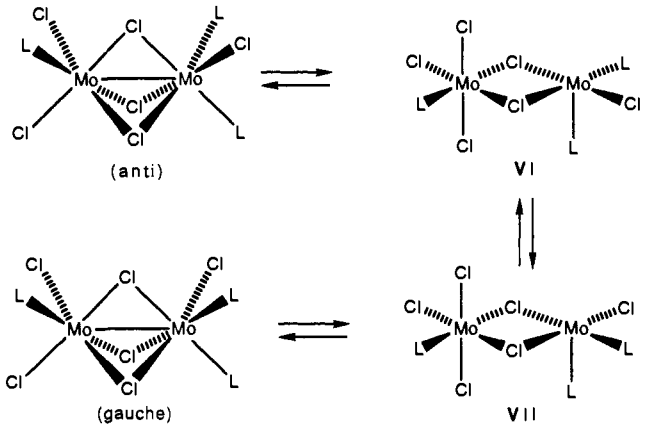

a hypothetical reaction pathway that produces an ESBO derivative with a different stereochemistry than ax,ax;eq,eq must be either thermodynamically unfavorable with respect to other reactions, or it must be followed by rapid isomerization of the product to the ax,ax;eq,eq isomer.

The observed reactivity pathways can be relatively easily explained based on the single assumption that there is a trans effect which results in faster substitution at positions trans to phosphine ligands with respect to position trans to chloride ligands, in analogy to what recently demonstrated for the ligand substitution reactions on mononuclear octahedral Mo(III) complexes.[6] It is also to be observed that the previously published structural data for *anti*-$Mo_2Cl_6(PR_3)_3$ molecules indicate a substantial trans influence on the Mo–(μ-Cl) bonds: the longer, thus presumably weaker, bonds are those located trans relative to phosphine ligands.[1,13,22]

As far as the isomerization reaction of the FSBO complexes is concerned, any Mo–(μ-Cl) bond can be broken and reformed after structural rearrangement of the coordination sphere around the five-coordinate center. The bonds that are broken more rapidly, however, are those located trans relative to phosphine ligands (bonds labeled 1, 5, and 6 in the anti isomer, **II**, and those labeled 7, 11, and 12 in the gauche isomer, **III**). By invoking the principle of microscopic reversibility, the reformation of a Mo–(μ-Cl) bond should also be more rapid if this bond is located

(20) (a) Cotton, F. A. *Polyhedron* **1987**, *6*, 667, and references therein. (b) Cotton, F. A.; Matusz, M.; Torralba, R. *Inorg. Chem.* **1989**, *28*, 1516. (c) Rh(III) edge-sharing dimers were prepared a long time ago, but their stereochemistry was not determined with certainty: Chatt, J.; Johnson, N. P.; Shaw, B. L. *J. Chem. Soc.* **1964**, 2508. Recent NMR studies have shown that these molecules possess an ax,ax;eq,eq stereochemistry.[19]

(21) (a) Babaian-Kibala, E.; Cotton, F. A.; Kibala, P. A. *Inorg. Chem.* **1990**, *29*, 4002. (b) Babaian-Kibala, E.; Cotton, F. A. *Inorg. Chim. Acta* **1991**, *182*, 77.

(22) Cotton, F. A.; Luck, R. L.; Son, K. *Inorg. Chim. Acta* **1990**, *173*, 131.

trans to a phosphine ligand. It can be seen that it is possible to convert the two isomers by breaking and reforming only bonds trans to phosphine ligands (see Scheme III). Thus, according to this scheme, it is not necessary to enter the ESBO manifold to induce rapid anti/gauche isomerization for the neutral FSBO $Mo_2Cl_6L_3$ compounds. It has to be observed here that the corresponding ionic FSBO $[Mo_2X_7L_2]^-$ complexes exhibit syn/gauche isomerization at a much slower rate,[12,14] consistent with the absence, in that case, of a pathway where both rupture and bond reformation steps occur at a site which is located trans to a phosphine ligand. We would also like to observe here that the anti/gauche isomerism has not been observed for FSBO compounds of Rh(III)[19] and W(III),[4] indicating that either the Mo–Cl bonds are more labile than W–X and Rh–X bonds or that there is a stronger thermodynamic preference for the anti isomer in Rh(III) and W(III) FSBO complexes.

Concerning the FSBO-to-ESBO transformation, intermediates similar to **VI** and **VII** in Scheme III can lead to formation of ESBO materials by simply adding a phosphine ligand to the available coordination site. However, only intermediates obtained by breaking bonds 1, 2, or 3 in **II** and 7, 8, or 9 in **III** will produce a material that contains two phosphine ligands per metal atom (rather than three on one metal and one on the other when starting from intermediates obtained by breaking bonds 4–6 or 10–12). The most straightforward pathway is the one starting with rupture of bond 1 in the anti isomer **II**, which is expected to be rapid since the bond is trans to a phosphine ligand, and leading directly to the thermodynamically most stable product (Scheme I). Presumably, the intermediate obtained by breaking bond 7 in the gauche isomer is also easily accessible in a kinetic sense, but perhaps the close contact between the two bulky L ligands in syn axial positions makes it thermodynamically less favorable. If any other ESBO product is obtained, it must rapidly isomerize to the ax,ax;eq,eq isomer since no other ESBO isomer accumulates in solution to such an extent to be observable by the NMR technique. Such an isomerization could occur through opening of the Mo_2Cl_2 bridge followed by rearrangement of the unsaturated (five-coordinate) metal and reclosure of the Mo_2Cl_2 ring. We observe, however, that such an isomerization pathway for the ESBO dimers (at least those that are heavily methyl substituted) would involve loss of the metal–metal interaction in the intermediate, which might impose energetic limitations. Thus, we prefer to adopt the view that ESBO products different than the ax,ax;eq,eq isomer are not produced to a significant level. In conclusion, the above scheme is consistent with the hypothesis of a higher reactivity of the anti vs the gauche FSBO dimer and suggests a selective addition of phosphine to the axial position of the ESBO product.

Homoleptic Edge-Sharing Dimers, $Mo_2Cl_6(PMe_xEt_{3-x})_4$: Nature of the Ground State and Effect of the Et/Me Ratio. As Figure 2 shows, the room temperature paramagnetic shifts increase with the Et/Me ratio. A point of interest for this study was a question we raised in our previous contribution.[1] On the basis of a simple group theoretical analysis, the ground states for a metal–metal bonded and for the corresponding nonbonded ESBO dimer are of a different symmetry type, thus an activation barrier may be expected for the interconversion of the two structures. We thus suggested[1] that it may be possible to observe both structures contemporarily in solution provided the two ground states have comparable energy (so as to give an observable population for each isomer) and the barrier to interconversion is high enough. Our synthetic studies of mixed methylethylphosphine ESBO derivatives were indeed carried out in search for a system having comparable ground state energies for bonded and nonbonded isomers.

It seems that the PMe_2Et and $PMeEt_2$ ESBO derivatives experience intermediate magnetic properties between those of the metal–metal bonded PMe_3 and the nonbonded PEt_3 derivatives, indicating that we are in fact at the crossover point between the two structural types. Unfortunately, pure solid materials could not be obtained for the reasons outlined above, thus preventing us from obtaining quantitative information from variable temperature magnetic susceptibility studies. However, according to theory,[23] the paramagnetic shift in the NMR spectrum is proportional to the magnetic susceptibility, thus the magnetic interactions in these materials can be qualitatively investigated by VT-NMR.

The data available to us (Figure 3) can in principle be interpreted in three possible ways: (i) with an equilibrium between two isomers, one with and one without a metal–metal bonding interaction, the metal–metal bonded isomer being prevalent for the methyl substituted complexes and the metal–metal nonbonded isomer being the dominant species for the more ethyl substituted complexes; (ii) the compounds are present as single isomers in solution and the metal–metal bonding interaction changes from very strong (PMe_3) through various degrees of intermediate (PMe_2Et and $PMeEt_2$) to very weak or nonexistent (PEt_3), whereas the magnetic interaction changes from a very strong antiferromagnetic coupling to a very weak one; (iii) the situation could be as described above in (ii), but, in addition, the strength of the magnetic and bonding interactions (that is the value of the coupling constant J and the metal–metal distance) might not be independent of temperature, for instance for the $PMeEt_2$ complex the metal–metal bond might be shorter and J might be higher at lower temperature.

Case (i) has recently been invoked to explain the observed temperature dependent ^1H NMR properties of compound $[Cp^*RuCl_2]_2$,[24] which are similar to those shown in Figure 3 for the PMe_3- and $PMe_2EtMo(III)$ complex. Two "deformational" isomers, one metal–metal bonded and one nonbonded, have been found to cocrystallize for this compound.[24] For our Mo(III) system, it appears more difficult to explain all experimental data with an isomer equilibrium. Firstly, if that were the case, the equilibrium must be very fast on the ^1H NMR time scale since a single set of peaks was observed for the $PMeEt_2$ compound (which should be the one with the closest match of ground state energies according to the data in Figure 3) down to ca. 180 K. Spin-orbit coupling may be invoked to rationalize a low barrier for the isomerization reaction. Secondly, the data for the $PMeEt_2$ compound indicate the predominance of the hypothetical nonbonded isomer at room temperature (i.e., a lower energy ground state for the nonbonded isomer). In that case, the paramagnetic shifts would be expected to increase upon lowering the temperature, contrary to what we observe.

If case (ii) is the valid one, the trends observed in Figure 3 must be in agreement with the corresponding variation of the magnetic susceptibility as a function of temperature for a single value of the metal–metal distance. The simplest description of the ground state for an antiferromagnetically coupled dimer is the standard Heisenberg–Dirac–Van Vleck (HDVV) model.[25] Curves for a selected number of J values have been calculated for two interacting $S = {}^3/_2$ spin systems and are shown in Figure 8. A comparison between Figure 3 and 8 shows similar qualitative trends, but for HDVV systems with an intermediate J value (−50 and −100 cm^{-1}) the relative variation of χ in the 200–300 K range is much smaller than the observed variation of paramagnetic shift for the $PMeEt_2$ complex. It is worth pointing out that, for a given compound, the *absolute* value of the paramagnetic shift can be related to the absolute value of the magnetic susceptibility only with difficulty, because the Fermi contact and dipole contributions depend on several geometric parameters.[23] However, in our case we are comparing paramagnetic shifts for the *same* type of proton in a series of compounds of identical geometry, thus the nuclei of interest are always located at approximately the same distance and relative position in space with respect to the dimolybdenum unit. Consequently, the variation of the paramagnetic shift *for the same type of proton* on going from one compound to another should reflect quite closely the variation of the magnetic susceptibility among the two compounds. The data in Figure 3 thus suggest that our dimers do not obey the HDVV model for a S_1

(23) Jesson, J. P. In *NMR of Paramagnetic Molecules*; La Mar, G. N., Horrocks, W. DeW., Jr., Holm, R. H., Eds.; Academic Press: New York, 1973; Chapter 1.
(24) Kölle, U.; Kossakowski, J.; Klaff, N.; Wasemann, L.; Englert, U.; Herberich, G. E. *Angew. Chem., Int. Ed. Engl.* **1991**, *30*, 690.
(25) O'Connor, C. J. *Prog. Inorg. Chem.* **1984**, *29*, 203.

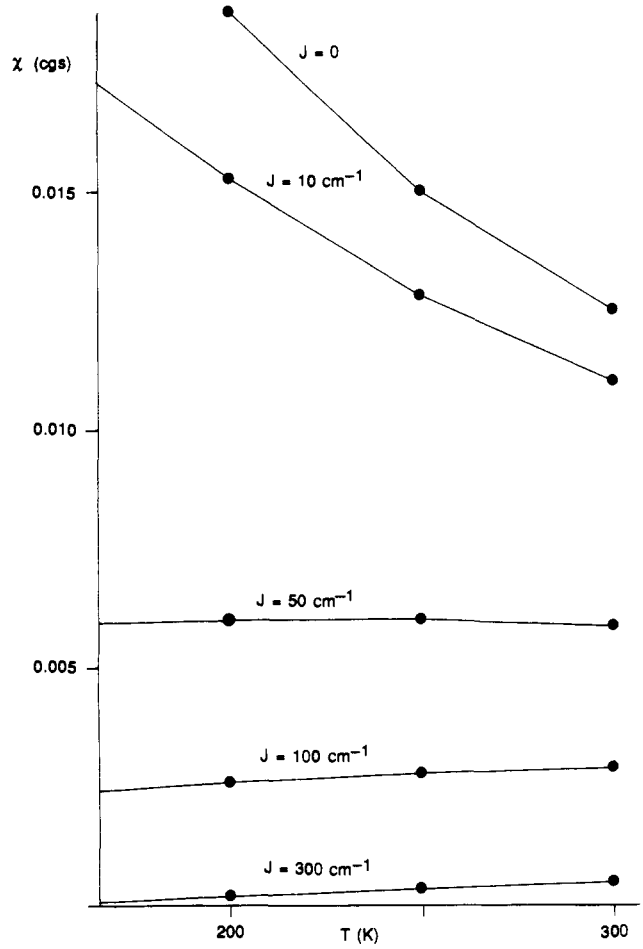

Figure 8. Calculated magnetic susceptibility for two antiferromagnetically coupled $S = 3/2$ systems that obey the HDVV model.[23]

$= S_2 = {}^3/_2$ system. Deviations from the HDVV model have been observed for other dinuclear compounds where the possibility exists for the formation of direct metal–metal bonds.[26] For our particular system, the relative strength of the metal–metal interaction in the order $\sigma > \pi > \delta$ is expected to distort the ideal Landê separation of the $S = 0$–3 spin levels for the B_{1u} ($\sigma^1\pi^1\delta^1\delta^{*1}\pi^{*1}\sigma^{*1}$) ground state (in ideal D_{2h} symmetry). Furthermore, for strong enough bonding interactions, other multiplets derived from the combination of the mononuclear octahedral states [e.g., B_{1g} ($\sigma^2\pi^1\delta^1\delta^{*1}\pi^{*1}$)] may become accessible or even lower in energy and contribute to reduce the effective magnetic moment at low temperature. A more detailed analysis of the electronic structure would require the experimental values of the magnetic susceptibility at various temperature, which will be very difficult to obtain for this particular system as outline above.

The data would also seem in qualitative agreement with a situation in which the metal–metal bond is temperature dependent, becoming relatively stronger as temperature decreases, i.e., case (iii). We are not aware that this situation is precedented in the literature.

The temperature dependence for compounds $Mo_2Cl_6(PEt_3)_3$-(ax-PMe_3) and $Mo_2Cl_6(PEt_3)_2(ax\text{-}PMe_3)_2$ (Figure 7) indicates that they both have magnetic properties intermediate between those of $Mo_2Cl_6(PMeEt_2)_4$ and $Mo_2Cl_6(PEt_3)_4$. For both compounds, the paramagnetic shift increases with a decrease of temperature in analogy to the homoleptic PEt_3 compound, but the behavior in these cases starts to significantly deviate from that predicted by the Curie law (e.g., $\Delta\delta$ proportional to $1/T$).

Effect of the Location of Me and Et Groups on the Paramagnetism of Edge-Sharing Bioctahedral Complexes. Qualitatively, the paramagnetism of mixed-phosphine ESBO complexes, i.e., $Mo_2Cl_6L_3(ax\text{-}L')$ and $Mo_2Cl_6L_2(ax\text{-}L')_2$, as indicated by the upfield shift of the phosphine α proton NMR resonances, increases as the Me/Et ratio decreases, in line with the results obtained for the homoleptic $Mo_2Cl_6(PMe_xEt_{3-x})_4$ derivatives described above. A comparison between different "substituent positional isomers" shows that the paramagnetism is sensitive to the distribution of the Me and Et groups among axial and equatorial positions. No clear trend, however, appears to emerge from a detailed analysis of the spectra.

For instance, compare the two isomeric compounds Mo_2Cl_6-$(PMe_3)_2(ax\text{-}PEt_3)_2$ and $Mo_2Cl_6(PEt_3)_2(ax\text{-}PMe_3)_2$, both containing six Me and six Et substituents. The first compound has the α proton resonances in the δ −6 to −7 range (peaks labeled e in Figure 4d), whereas the second one has the PMe_3 resonance at δ −17 and the PEt_3 methylene resonance in the δ −25 to −27 range (see Results). From this comparison, it would be tempting to conclude that the greater paramagnetic shifts are obtained when Et groups are located in equatorial positions. Other comparisons seem to agree with this view, for instance the compounds $Mo_2Cl_6(PMe_3)_3(ax\text{-}PMeEt_2)$ and $Mo_2Cl_6(PMe_2Et)_2(ax\text{-}PMe_3)_2$, both with a Me/Et ratio of 10:2, show shifts in the δ −1 to −3 range for the first one (no equatorial Et groups, Figure 5a) and at least one resonance upfield of δ −4 for the second one (two equatorial Et groups, resonance labeled B in Figure 5d). However, for compounds $Mo_2Cl_6(PMe_2Et)_4$ and $Mo_2Cl_6(PMe_3)_2(ax\text{-}PMeEt_2)_2$, both having Me/Et = 8:4, an opposite trend is observed: shifts are in the δ −4 to −5.5 for the first one (two equatorial Et groups, Figure 2b) and in the δ −6 to −8 region for the second one (no equatorial Et group, Figure 5a). And very little difference is observed between the ranges for compounds $Mo_2Cl_6(PMe_3)_3$-(ax-PEt_3) (resonances labeled c in Figure 4) and Mo_2Cl_6-$(PMe_2Et)_3(ax\text{-}PMe_3)$ (resonances labeled A in Figure 5d), both having Me/Et = 9:3. It has to be reemphasized that these considerations are based on the validity of Scheme I, i.e., selective attack of phosphine on the FSBO compound to end up in an axial position in the resulting ESBO compound, and on the validity of the assignments of the ^1H NMR resonances given in Results.

Trans Effect of PMe_3 vs PEt_3. The observations presented in Results provide indirect experimental evidence for an increasingly stronger trans effect of PMe_xEt_{3-x} as the value of x increases. According to Scheme II, the relative rate of formation of $Mo_2Cl_6L_2(ax\text{-}L')_2$ vs the rate of formation of $Mo_2Cl_6L_3(ax\text{-}L')$ should increase with the trans directing ability of L′ vs that of L. Figure 4 (L′ = PEt_3, L = PMe_3) and Figure 5a (L′ = $PMeEt_2$, L = PMe_3) show that the $Mo_2Cl_6L_2(ax\text{-}L')_2$ products are obtained much more slowly than the $Mo_2Cl_6L_3(ax\text{-}L')$ products indicating, respectively, the order of trans directing ability $PMe_3 > PEt_3$ and $PMe_3 > PMeEt_2$. On the other hand, Figure 5 (parts c and d) (L′ = PMe_3, L = PMe_2Et) and Figure 6 (L′ = PMe_3, L = PEt_3) show that the compounds with two ax-L′ ligands are produced at a rate comparable with that of the primary products that contain only one ax-L′ ligand, consistent with the orders $PMe_3 > PMe_2Et$ and $PMe_3 > PEt_3$, respectively.

A Possible Steric Effect? Coming back to a point raised in the Introduction, we can discuss the electronic and steric influence of the phosphine substituents on the nature of the ground state for the Mo(III) ESBO derivatives in the light of the new results presented in this contribution. The dominance of the electronic influence of the phosphine substituents on the stabilization of the metal–metal bond had already been seriously questioned, if not completely dismissed, by the observation that the stronger donating PEt_3 ligand (with respect to PMe_2Ph) should expand more the metal orbitals favoring overlap and formation of the metal–metal bond, whereas in reality the PEt_3 structue is nonbonded and the PMe_2Ph structure is bonded. The present study indicates that the dramatic change occurs between two electronically even more similar phosphines, e.g., PMe_3 and PEt_3. Is it possible that the difference between these two phosphines is sufficient to tip the balance of the system through their electronic influence on the stabilization of the ground state for the nonbonded structure (i.e., through their different nephelauxetic parameter)? This question cannot, of course, be answered based on the results obtained in this study, and an investigation of the relative nephelauxetic parameter of PMe_3 and PEt_3 has never been reported to the best of our knowledge.

Certainly, the difference between PMe_3 and PEt_3 appears to be greater in terms of steric parameters (cone angles: PMe_3, 118; PEt_3, 132) than in terms of electronic parameters (ν for $Ni(CO)_3L$: PMe_3, 2064.1; PEt_3, 2061.7).[27] It has been argued before that the greatest steric interaction in ESBO complexes is that between the ligands in relative syn axial positions.[28] If this is true, the greater paramagnetism of $Mo_2Cl_6(PEt_3)_2(ax\text{-}PMe_3)_2$ with respect to the isomeric $Mo_2Cl_6(PMe_3)_2(ax\text{-}PEt_3)_2$ would argue against the importance of steric effects (the *ax*-Cl-*ax*-PEt_3 interaction in the latter compound should be more destabilizing than the *ax*-Cl-*ax*-PMe_3 interaction in the former one). However, this syn–ax interaction should be important only when both ligands have lone pairs.[28] In our case, only one of them (the Cl ligand) does. Furthermore, as one reviewer suggests, the steric effect may be transmitted more strongly in the equatorial position, based on the following arguments: it is known that the deviation of an octahedral angle from 90° causes an opposite deviation of the corresponding trans angle through a metal orbital rehybridization, a phenomenon that may be termed "reverse scissoring effect". For example, in the $Mo_2Cl_6(PMe_2Ph)_4$ structure,[1] the angles in the $Mo_2Cl_4P_2$ equatorial core (cf. **VIII**) are α, 86.42 (5)°; β, 109.69 (5)°; γ, 107.36 (5)°; δ, 96.83 (5)°. The obtuse β and γ angles are enforced by the metal–metal bonding interaction. By virtue of the reverse scissoring effect, the obtuse β induces an acute α, but on the other hand δ is nevertheless obtuse, indicating a steric interaction between the two equatorial PMe_2Ph ligands. Since PEt_3 is even bulkier than PMe_2Ph (cone angles: 132° vs 122°), this may require a larger value for δ, which in turn would induce a smaller angle γ resulting in the metal–metal interaction to be weakened. The δ angle in the nonbonded $Mo_2Cl_6(PEt_3)_4$ complex is 101.0 (2)°,[2] but this number alone does not prove the steric argument since it is not established what is the cause and what is the effect. In other words, it could be that the larger δ angle observed in the PEt_3 compound is *the result* of the compound lacking a metal–metal interaction and therefore having a smaller γ angle (82.7 (1)°).

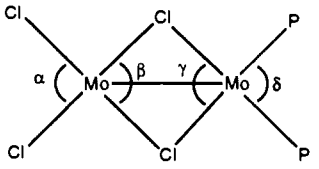

VIII

In order to address this steric argument, we are carrying out a series of semiempirical MO calculations on this system for different values of α, β, γ, and δ. These will be reported in the future. For the moment, we limit ourselves to comparisons between the published solid state structures of *ax,ax,eq,eq*-$W_2Cl_6L_4$ and *eq,eq,eq,eq*-$Zr_2Cl_6L_4$ where L is either PMe_2Ph or PEt_3 in each case. These are the only pairs of structurally characterized ESBO compounds that are identical in all respects except for a change of L from PMe_2Ph to PEt_3. For $W_2Cl_6(PMe_2Ph)_4$,[29] the W–W (Å), γ (deg), and δ (deg) parameters are, respectively, 2.6950 (3), 109.75 (4), and 91.87 (4), whereas for $W_2Cl_6(PEt_3)_4$ the same parameters are 2.7397 (7), 109.2, and 92.5.[4,30] Unlike the corresponding Mo(III) systems, both W(III) dimers show a metal–metal interaction, most probably due to the increase of metal–metal bond strength on going from Mo to W. There is a slight increase of δ on going from the PMe_2Ph to the PEt_3 complex, which is paralleled by a decrease of γ and by an increase of the W–W distance, as expected on the basis of the steric arguments discussed above. On the other hand, these data show that two PEt_3 ligands in mutually cis positions can achieve a bond angle as low as 92.5°. The corresponding Zr–Zr (Å), γ (deg), and δ (deg) parameters for the two $Zr_2Cl_6L_4$ (L = PMe_2Ph, PEt_3) compounds are 3.127 (1), 104.26 (8), and 96.19 (8) for the PMe_2Ph compound and 3.169 (1), 102.81 (5), and 96.02 (6)° for the PEt_3 compound.[18b] In this case, therefore, the slightly longer Zr–Zr bond is not paralleled by a larger angle between the two bulkier phosphine ligands.

Summary and Conclusions

The present investigation further advances our understanding of the rich and complex coordination chemistry and stereochemistry of octahedral Mo(III) complexes. This has been made possible by the use of the paramagnetic ^1H NMR technique. In fact, for the α protons of phosphine ligands attached to molybdenum centers whose magnetic properties vary continuously between those of diamagnetic and magnetically diluted $S = {}^3/_2$ systems, the chemical shift varies continuously in the δ +1 to −30 range at room temperature, a range that is devoid of any other resonance. Thus, the observed pattern of resonances gives precise information about the chemical identity and stereochemistry of the compounds present. This situation can be compared with the application of IR spectroscopy in the 2200–1700-cm^{-1} region for the selective investigation of transition metal carbonyl complexes but, in addition to obtaining information on the stoichiometry and stereochemistry, additional information on the magnetic properties can be obtained from the temperature dependence of the chemical shifts.

For the particular case of the edge-sharing bioctahedral Mo(III) complexes of structure **I**, the present investigation has given information on the nature of the ground state as a function of type and relative position of phosphine substituents. A dramatic change of magnetic properties has been observed by the simple replacement of PMe_3 with PEt_3 in the homoleptic $Mo_2Cl_6L_4$ compound. Variable temperature ^1H NMR investigations of the $Mo_2Cl_6(PMe_xEt_{3-x})_4$ derivatives seem to suggest that a fast equilibrium between two different isomeric forms of the compound (one with and one without a Mo–Mo direct bonding interaction) is not present and appears most consistent with an antiferromagnetic interaction which considerably deviates from the classical Heisemberg–Dirac–Van Vleck model. Finally, the investigation of mixed-phosphine ESBO compounds has shown a regioselective attack of phosphine L′ to FSBO $Mo_2Cl_6L_3$ materials and has indirectly provided evidence for a stronger trans effect of more methyl substituted PMe_xEt_{3-x} ligands. Simple mechanistic considerations suggest that the regioselective attack results in the formation of $Mo_2Cl_6L_3(ax\text{-}L')$ rather than its isomer where L′ occupies an equatorial position.

A more detailed investigation of the ground state of these materials is not possible because of their tendency to thermally decompose by ligand disproportionation, which prevents their isolation in the pure state. The formation of single crystals for a solid state structural investigation, which was successful for the $Mo_2Cl_6L_4$ (L = PMe_2Ph,[1] PEt_3[2]) compounds, has so far failed in our hands for the homoleptic $PMeEt_2$ compound and for the mixed phosphine $Mo_2Cl_6(PEt_3)_{4-n}(ax\text{-}PMe_3)_n$ (n = 1, 2) complexes, which are the systems with the most interesting magnetic properties according to the variable temperature NMR studies. Future studies will be directed to search for other dinuclear systems that show an analogous dependence of the ground state properties on the type and relative position of substituents and that are at the same time thermally stable.

Acknowledgment. We are grateful to the National Science Foundation for a PYI Award to R.P. (CHE-9058375) and for support.

(26) Stranger, R.; Smith, P. W.; Grey, I. E. *Inorg. Chem.* **1989**, *28*, 1271.
(27) Tolman, C. A. *Chem. Rev.* **1977**, *77*, 313.
(28) Shaik, S.; Hoffmann, R.; Fisel, C. R.; Summerville, R. H. *J. Am. Chem. Soc.* **1980**, *102*, 4555.
(29) Cotton, F. A.; Mandal, S. K. *Inorg. Chem.* **1992**, *31*, 1267.
(30) The angular parameters were provided in a personal communication by Prof. M. H. Chisholm.